trend = 0.38). There was no significant effect of the interaction between *APOE*-ϵ4 carrier status and rs3851179 genotype on the risk of LOAD (*P* for interaction = 0.68).

Discussion

In the present study, we found that the marker SNP for the *PICALM* gene (rs3851179) was significantly associated with LOAD in the Japanese population. Although the association of this SNP has already been replicated in populations of European descent (Carrasquillo *et al.*, 2010; Corneveaux *et al.*, 2010; Jun *et al.*, 2010; Kamboh *et al.*, 2010), this is, to our knowledge, the first association study to show significant associations between *PICALM* and LOAD in other ethnicities.

Although rs3851179 is located at 88.5 kb upstream from the *PICALM* gene and 87 kb upstream from the *EED* gene, the HapMap data indicate that this SNP is located in the linkage disequilibrium block, which includes the *PICALM* gene, but not the *EED* gene, in populations of both European and Japanese descent (data not shown). Besides, the precise role of the *PICALM* gene product in LOAD development is unclear. This product is expressed in all tissue types, with a prominent expression in neurons, and plays an important role in the trafficking of vesicle-associated membrane protein 2, which is crucial to neuronal function and memory formation (Harel *et al.*, 2008; Bettens *et al.*, 2010). Meanwhile, the *PICALM* gene product might play a role in amyloid precursor protein processing through the endocytic pathway (Harold *et al.*, 2009; Bettens *et al.*, 2010). Therefore, functional variants in *PICALM* may possibly affect the changes in synaptic function or endocytosis of the amyloid precursor protein, resulting in the susceptibility for LOAD. Further functional studies of *PICALM* could lead toward a better understanding of this issue.

In this study, we could not find significant associations between six susceptibility genes and LOAD. There is a large difference in the minor allele frequency (MAF) of rs6656401 (*CR1*) between European and Japanese populations (MAF = 0.23 for Europeans and 0.04 for Japanese). This low MAF in Japanese markedly decreased the statistical power to 0.32 in this study. Meanwhile, our study had a marginal statistical power of two SNPs [0.79 for rs744373 (*BIN1*) and 0.76 for rs11136000 (*CLU*)], but no significant associations after adjustment for age and sex. One reason for this may be our relatively small case–control samples. Another is that, because the LOAD cases and controls were all individuals of Japanese descent, the genetic heterogeneity among different ethnicities could have weakened the associations with these two SNPs.

In contrast, although our samples had sufficient statistical power (> 0.80), we found no significant associations in two SNPs: rs237311 (*GAB2*) and rs597668 (*EXOC3L2*). This might be because of genetic differences between populations. On the basis of the HapMap data, linkage disequilibrium blocks surrounding these SNPs differ between Europeans and Japanese. Miyashita *et al.* (2009) also reported a difference in the linkage disequilibrium block of the *GAB2* gene between European and Japanese populations. Therefore, it is possible that the unknown causative variants and the marker SNPs are tightly linked in populations of European descent, whereas such linkages may be weak or nonexistent in the Japanese population. Another possibility is that the *GAB2* association is detectable only with stratification by *APOE*-ϵ4 carrier status (Liang *et al.*, 2011). However, we could not find a significant association between rs237311 and LOAD in either *APOE*-ϵ4 carriers or noncarriers (OR 0.93, 95% CI 0.68–1.28 for *APOE*-ϵ4 carriers; OR 0.85, 95% CI 0.69–1.05 for *APOE*-ϵ4 noncarriers). Meanwhile, we failed to find a significant association between rs597668 and LOAD after adjustment for age, sex, and APOE genotype (OR 0.97, 95% CI 0.81–1.17). Lambert *et al.* (2011) and Carrasquillo *et al.* (2011) also reported a nonsignificant association between the *EXOC3L2* gene and LOAD after adjustment for age, sex, and the *APOE*-ϵ4 genotype.

Conclusion

We found the genetic variants in *APOE* and *PICALM* to be associated with LOAD in the Japanese population. Together with published data on populations of European descent, our data indicate that *APOE* and *PICALM* could be the susceptibility genes for LOAD in several ethnic populations. Further investigations are required to establish more reliable associations between these genes and LOAD.

Acknowledgements

The authors thank the patients with Alzheimer's disease and residents of Hisayama for their participation; all members of the Division of Health and Welfare of Hisayama for their cooperation; many members of the Hisayama study for assistance. For collecting clinical samples, the authors thank K. Sasaki, A. Ohashi, N. Oribe, and member of the Department of Neuropsychiatry (Kyushu University Hospital); M. Takita (Takita Memory Mental Clinic); S. Maki (Maki Hospital); M. Saito (Yahata Kosei Hospital); N. Ikko (Yukuhashi Kinen Hospital); R. Nakagawa (Ureshino Onsen Hospital); K. Serikawa (Monowasure Mental Clinic); T. Toyonaga (Iizuka Kinen Hospital); M Hayashi (Asakura Kinen Hospital); N. Fujikawa (Fujikawa Medicare Clinic); A. Notomi (Imazu Red Cross Hospital); Y. Sumita (Sumita Hospital); M. Sakurai (Shinmoji Hospital); S. Ohara (Minamigaoka Hospital); K. Nishimaru (Yoshizuka Hayashi Hospital); S. Hisano (Kanenokuma Hospital); M. Ito (Nogata Nakamura Hospital); Y. Hasuo (Wakasugi Hospital); F. Hattori (Nagao Hospital); I. Fujii (Shineikai Hospital); Y. Tanizaki (Kotake Town Hospital). They also thank the staff of Laboratory for

Genotyping Development, Center for Genomic Medicine, RIKEN, for their contribution to the completion of our study.

This study was supported in part by the Ministry of Education, Culture, Sports, Science and Technology of Japan, and a Health and Labour Sciences Research Grant of the Ministry of Health, Labour and Welfare of Japan (Comprehensive Research on Aging and Health: H20-Chouju-004).

Conflicts of interest

There are no conflicts of interest.

References

American Psychiatric Association (1987). *Diagnostic and Statistical Manual of Mental Disorders.* 3rd ed., revised. ed. Washington, DC: American Psychiatric Association.

Beecham GW, Martin ER, Li YJ, Slifer MA, Gilbert JR, Haines JL, *et al.* (2009). Genome-wide association study implicates a chromosome 12 risk locus for late-onset Alzheimer disease. *Am J Hum Genet* **84**:35–43.

Belbin O, Dunn JL, Ling Y, Morgan L, Chappell S, Beaumont H, *et al.* (2007). Regulatory region single nucleotide polymorphisms of the apolipoprotein E gene and the rate of cognitive decline in Alzheimer's disease. *Hum Mol Genet* **16**:2199–2208.

Bettens K, Sleegers K, Van Broeckhoven C (2010). Current status on Alzheimer disease molecular genetics: from past, to present, to future. *Hum Mol Genet* **19**:R4–R11.

Carrasquillo MM, Zou F, Pankratz VS, Wilcox SL, Ma L, Walker LP, *et al.* (2009). Genetic variation in PCDH11X is associated with susceptibility to late-onset Alzheimer's disease. *Nat Genet* **41**:192–198.

Carrasquillo MM, Belbin O, Hunter TA, Ma L, Bisceglio GD, Zou F, *et al.* (2010). Replication of CLU, CR1, and PICALM associations with Alzheimer disease. *Arch Neurol* **67**:961–964.

Carrasquillo MM, Belbin O, Hunter TA, Ma L, Bisceglio GD, Zou F, *et al.* (2011). Replication of BIN1 association with Alzheimer's disease and evaluation of genetic interactions. *J Alzheimer Dis* **24**:751–758.

Corneveaux JJ, Myers AJ, Allen AN, Pruzin JJ, Ramirez M, Engel A, *et al.* (2010). Association of CR1, CLU and PICALM with Alzheimer's disease in a cohort of clinically characterized and neuropathologically verified individuals. *Hum Mol Genet* **19**:3295–3301.

Harel A, Wu F, Mattson MP, Morris CM, Yao PJ (2008). Evidence for CALM in directing VAMP2 trafficking. *Traffic* **9**:417–429.

Harold D, Abraham R, Hollingworth P, Sims R, Gerrish A, Hamshere ML, *et al.* (2009). Genome-wide association study identifies variants at CLU and PICALM associated with Alzheimer's disease. *Nat Genet* **41**: 1088–1093.

Ikram MA, Liu F, Oostra BA, Hofman A, van Duijn CM, Breteler MM (2009). The GAB2 gene and the risk of Alzheimer's disease: replication and meta-analysis. *Biol Psychiatry* **65**:995–999.

Jun G, Naj AC, Beecham GW, Wang LS, Buros J, Gallins PJ, *et al.* (2010). Meta-analysis confirms CR1, CLU, and PICALM as Alzheimer disease risk loci and reveals interactions with APOE genotypes. *Arch Neurol* **67**:1473–1484.

Kamboh MI, Minster RL, Demirci FY, Ganguli M, Dekosky ST, Lopez OL, *et al.* (2012). Association of CLU and PICALM variants with Alzheimer's disease. *Neurobiol Aging* **33**:518–521.

Kubo M, Hata J, Ninomiya T, Matsuda K, Yonemoto K, Nakano T, *et al.* (2007). A nonsynonymous SNP in PRKCH (protein kinase C eta) increases the risk of cerebral infarction. *Nat Genet* **39**:212–217.

Lambert JC, Heath S, Even G, Campion D, Sleegers K, Hiltunen M, *et al.* (2009). Genome-wide association study identifies variants at CLU and CR1 associated with Alzheimer's disease. *Nat Genet* **41**:1094–1099.

Lambert JC, Zelenika D, Hiltunen M, Chouraki V, Combarros O, Bullido MJ, *et al.* (2011). Evidence of the association of BIN1 and PICALM with the AD risk in contrasting European populations. *Neurobiol Aging* **32**:e11–e15.

Liang WS, Chen K, Lee W, Sidhar K, Corneveaux JJ, Allen AN, *et al.* (2011). Association between GAB2 haplotype and higher glucose metabolism in Alzheimer's disease-affected brain regions in cognitively normal APOEepsilon4 carriers. *Neuroimage* **54**:1896–1902.

McKhann G, Drachman D, Folstein M, Katzman R, Price D, Stadlan EM (1984). Clinical diagnosis of Alzheimer's disease: report of the NINCDS-ADRDA Work Group under the auspices of Department of Health and Human Services Task Force on Alzheimer's Disease. *Neurology* **34**:939–944.

Miyashita A, Arai H, Asada T, Imagawa M, Shoji M, Higuchi S, *et al.* (2009). GAB2 is not associated with late-onset Alzheimer's disease in Japanese. *Eur J Hum Genet* **17**:682–686.

Ohara T, Doi Y, Ninomiya T, Hirakawa Y, Hata J, Iwaki T, *et al.* (2011). Glucose tolerance status and risk of dementia in the community: the Hisayama Study. *Neurology* **77**:1126–1134.

Ohnishi Y, Tanaka T, Ozaki K, Yamada R, Suzuki H, Nakamura Y (2001). A high-throughput SNP typing system for genome-wide association studies. *J Hum Genet* **46**:471–477.

Purcell S, Cherny SS, Sham PC (2003). Genetic Power Calculator: design of linkage and association genetic mapping studies of complex traits. *Bioinformatics* **19**:149–150.

Reiman EM, Webster JA, Myers AJ, Hardy J, Dunckley T, Zismann VL, *et al.* (2007). GAB2 alleles modify Alzheimer's risk in APOE epsilon4 carriers. *Neuron* **54**:713–720.

Seshadri S, Fitzpatrick AL, Ikram MA, DeStefano AL, Gudnason V, Boada M, *et al.* (2010). Genome-wide analysis of genetic loci associated with Alzheimer disease. *JAMA* **303**:1832–1840.

Slooter AJ, Cruts M, Kalmijn S, Hofman A, Breteler MM, Van Broeckhoven C, *et al.* (1998). Risk estimates of dementia by apolipoprotein E genotypes from a population-based incidence study: the Rotterdam Study. *Arch Neurol* **55**:964–968.

OPEN ACCESS Freely available online

PLoS one

Minocycline Modulates Human Social Decision-Making: Possible Impact of Microglia on Personality-Oriented Social Behaviors

Takahiro A. Kato[1,2*☯], Motoki Watabe[3*☯], Sho Tsuboi[4], Katsuhiko Ishikawa[5], Kazuhide Hashiya[5], Akira Monji[1], Hideo Utsumi[2], Shigenobu Kanba[1]

1 Department of Neuropsychiatry, Graduate School of Medical Sciences, Kyushu University, Fukuoka, Japan, **2** Innovation Center for Medical Redox Navigation, Kyushu University, Fukuoka, Japan, **3** Graduate School of Economics, Waseda University, Waseda, Japan, **4** Department of Psychology, Graduate School of Letters, Kyoto University, Kyoto, Japan, **5** Graduate School of Human-Environment Studies, Kyushu University, Fukuoka, Japan

Abstract

Background: Microglia, one of the glial cells, play important roles in various brain pathologies including psychiatric disorders. In addition, microglia have recently been proved to monitor synaptic reactions via direct-touching even in normal brain. Human microglia may modulate various social/mental functions, while microglial social/mental roles remain unresolved especially in healthy humans. There is no known drug with the specific effect of modulating microglia. Therefore, using minocycline, a tetracycline antibiotic and the most famous microglial inhibitor, is one of the best alternative approaches to clarify microglial functions on human social/mental activities.

Methodology/Principal Findings: We conducted a double-blind randomized trial of trust game, a monetary decision-making experiment, with ninety-nine human adult males who decided how much to trust an anonymous partner after a four-day administration of minocycline. Our previous pilot trial indicated a positive effect of minocycline, while the underlying mechanisms were not clarified. Therefore, in this trial with larger samples, we additionally measured the effects of anxiety and personality. The monetary score in trust game was significantly lower in the minocycline group. Interestingly, participants' ways of decision-making were significantly shifted; cooperativeness, one component of personality, proved to be the main modulating factor of decision-making in the placebo group, on the other hand, the minocycline group was mainly modulated by state anxiety and trustworthiness.

Conclusions/Significance: Our results suggest that minocycline led to more situation-oriented decision-making, possibly by suppressing the effects of personality traits, and furthermore that personality and social behaviors might be modulated by microglia. Early-life events may activate human microglia, establish a certain neuro-synaptic connection, and this formation may determine each human's personality and personality- oriented social behaviors in later life. To explore these mechanisms, further translational research is needed.

Trial Registration: UMIN clinical trial center UMIN000004803

Citation: Kato TA, Watabe M, Tsuboi S, Ishikawa K, Hashiya K, et al. (2012) Minocycline Modulates Human Social Decision-Making: Possible Impact of Microglia on Personality-Oriented Social Behaviors. PLoS ONE 7(7): e40461. doi:10.1371/journal.pone.0040461

Editor: Frank Krueger, George Mason University/Krasnow Institute for Advanced Study, United States of America

Received April 1, 2012; **Accepted** June 7, 2012; **Published** July 13, 2012

Funding: This work was financially supported by Grant-in-Aid from the Japan Society for the Promotion of Science (JSPS) to Dr. Kato, Dr. Watabe, Dr. Hashiya, Dr. Monji, Dr. Utsumi and Dr. Kanba, and a JSPS Research Fellow Grant to Dr. Tsuboi. The funders had no role in study design, data collection and analysis, decision to publish, or preparation of the manuscript.

Competing Interests: All the authors have declared that no competing interests exist.

* E-mail: takahiro@npsych.med.kyushu-u.ac.jp (TAK); motokiw@gmail.com (MW)

☯ These authors contributed equally to this work.

Introduction

Microglia are one of the glial cells with immunological/inflammatory functions, and contribute to various brain pathologies; not only in neurodegenerative diseases [1,2,3] but also in psychiatric disorders such as schizophrenia and autism [4,5,6]. Minocycline, a tetracycline antibiotic, is known as the most famous microglial inhibitor [7], which has recently been applied to brain diseases such as stroke and neurodegenerative diseases [8,9]. In addition, minocycline has been suggested to be an effective drug for psychiatric disorders [10,11]. These reports suggest that inhibiting microglial activation may modulate human social and mental activities, and rodent studies have indicated this possibility [12,13].

Rodent microglia have recently been shown to monitor synaptic reactions via direct-touching not only in pathological brain but also in normal brain [14,15,16,17], and have proved to play important roles in normal brain development such as synaptic pruning [18]. Neurons and neuronal networks including synapses have been dominantly believed to play crucial roles in human social/mental activities. The above-mentioned evidence indicates

that human microglia may modulate various social/mental functions, while microglial social/mental roles continue to remain unresolved especially in healthy humans.

There is no known drug with the specific effect of modulating microglia. Therefore, using minocycline, a tetracycline antibiotic and the most famous microglial inhibitor, is one of the best alternative approaches to clarify microglial functions on human social/mental activities. One human study suggests that minocycline attenuates the subjective reward effects of dextroamphetamine [19], while, to our knowledge, the effects of minocycline on human social/mental activities are not well understood.

Crockett et al have revealed that serotonin modulates behavioral reactions to unfairness, via a monetary decision-making game with healthy volunteers who were administered tryptophan-depleted amino acid which induces lower serotonin levels [20]. In order to measure human social/mental activities, these monetary decision-making experiments have been actively applied because such experiments enable the analysis of the interaction between social/mental activities and actual social behaviors [21,22]. Pharmacology-based neuro-economic research is showing that human social behaviors are modulated by neurotransmitters such as serotonin and oxytocin [20,23,24,25]. In addition, a significant link has recently been reported between the dopamine D4 receptor gene and fairness preference in ultimatum game [26]. However, the pharmacological interaction of social decision-making beyond neurotransmitters remains to be clarified [27].

As a first step in this direction, we recently conducted a pilot experiment with trust game, one of the decision-making experiments, with minocycline [28]. The forty-nine participants, healthy adult humans, made a monetary decision about whether or not to trust an anonymous partner after a four-day oral administration of minocycline or placebo. The minocycline group showed a strong and positive correlation between their scores in trust game and their pre-evaluation scores in others' trustworthiness, but the placebo group did not. These pilot data have suggested that inhibitory effects of microglial activation may sharpen a sense of trust in social behavior, and this effect would enhance situation-oriented behaviors according to immediate social situations. In trust game, a player's optimal decision depends on his/her prediction about the other player's decision. Thus, social environment, including the other's behavior, determines what behavior the player should take. In our actual life, however, our decisions are determined not only by social environment but also by our fundamental mental factors such as temperament and character (i.e. personality), which are independent from situational factors and may strongly impact on decision-making. These factors may act as a "noise" in trust game and during similar human decision-making situations [29]. Our pilot data demonstrated that only the minocycline group showed situation- oriented decision-making, which suggests that microglia may be inducing the "noise" consistently and inhibiting microglial activation could reduce this "noise" effect. However, the underlying mechanisms of "noise" were not clarified in our previous trial [28], thus the next appropriate step is the measurement of the effects of not only trustworthiness but also anxiety and personality.

Therefore, to clarify the microglial "noise" effect during human social decision-making, we newly explored whether anxiety and personality as a "noise" influences outcomes of trust game on humans with minocycline or placebo. To improve the small sample size and the weaker statistical power of our previous trial, we newly conducted the trial with larger samples (about one hundred participants).

Methods and Materials

The protocol for this trial and supporting CONSORT checklist are available as supporting information; see Checklist S1, Protocol S1 and Protocol S2. This double-blind randomized study was approved by the Kyushu University Ethical Committee under the administration of the UMIN clinical trial center (**UMIN000004803**). All the participants of the present experiment, which was conducted in December 2010, were unique to this study and differ from the previous participants who enrolled in an earlier experiment in March 2010 under the administration of the UMIN clinical trial center (UMIN000003281: published in Watabe et al. Psychopharmacology 2012). Flow diagram of this study is listed on **Figure 1**. All participants gave written informed consent to participate after a complete description of the study. Participants were administered minocycline or placebo for four days, after which they played a trust game with an anonymous partner.

Subjects

Participants were recruited by advertisements on campus. Inclusion criterion was as follows; healthy adult males from 20 to 30 years old who can obtain informed consent. Exclusion criteria were the following five items; 1) those who have had side effects to antibiotics including minocycline, 2) those who have severe heart, liver or kidney disease, 3) those who have a tendency to develop allergies, and 4) those who have been diagnosed with psychiatric disorders. Their mental and physical health was confirmed by interview with a psychiatrist (TAK). All the participants were qualified for this study (**Table S1**).

Drug Administration

Participants received a sheet describing their detailed dosing schedule. They were then asked to write the exact time of every dosing, and to submit every capsule package as evidence of dosing. Participants started to take a capsule in the evening of the first day and twice daily (morning and evening) for four days afterward. On the day of the game experiment (the fifth day), they were instructed to take the last capsule three-hours prior to the appointment time for the experiment so that all participants played the trust game under the similar drug effect. Each capsule contained 100 mg minocycline (in the treatment group) or 100 mg lactose (in the placebo group). This minocycline dose (200 mg/day) is within the range of the usual daily dose used for treatment of infections [30], and this dose has also been applied in recent clinical trials [10,19]. Participants were randomly assigned to the treatment group or to the placebo group in advance, with a double-blind procedure.

Procedure

Prior to drug administration, participants completed a set of questionnaires (details in **Scales**). After four days of drug administration, participants were interviewed by physicians regarding side effects, other medications, and adherence to the drug administration protocol. They then played a trust game [21] and responded to the same set of questionnaires they had completed before administration.

Trust Game

Figure 2 shows the structure of trust game. In this two-player game, each player was initially given 1300 JPY (nine hundred JPY had been used in our previous trial [28], but to let participants recognized clearer incentive and make their decisions more seriously, we used 1300 JPY (about 15 USD) in this new trial so

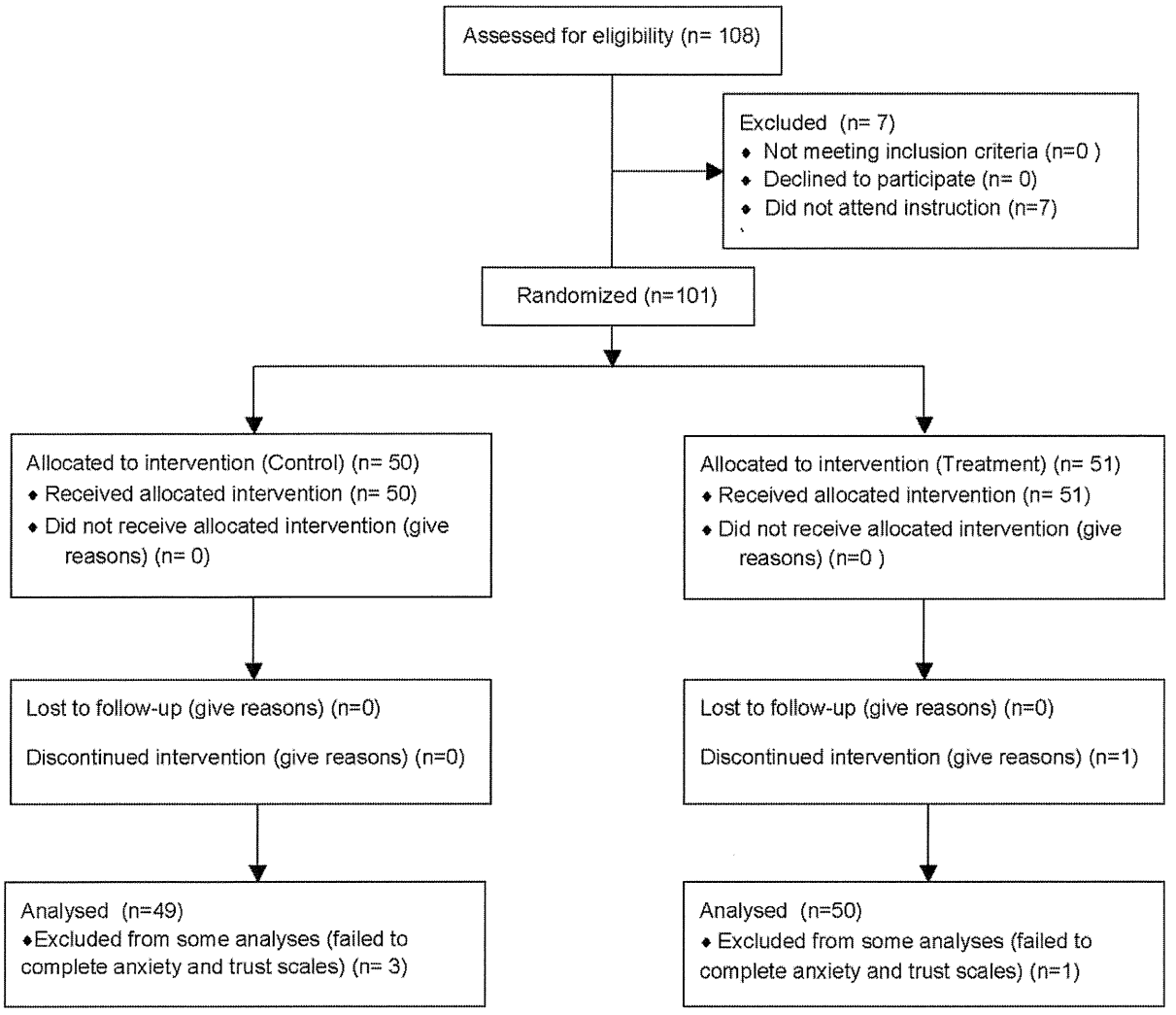

Figure 1. Flow Diagram of This Study.
doi:10.1371/journal.pone.0040461.g001

that we can obtain more reliable behavioral data). The first player then decided how much of the 1300 JPY to give to the second player. The second player then went to another room, where the amount of money given to him by the first player was tripled. The second player then decided whether to split his money equally with the first player or to take all of his money. In this experiment, all the participants were actually assigned to be the first player. The first player's decision as to how much money to give to the second player is thought to be the first player's level of trust in his partner. The amount of money given was expected to be a behavioral measure of the first player's trustfulness.

In this experiment, participants had no information about the partner except that he was male. The participants thus were likely to have made their decisions based primarily on how much they trusted others in general. All the participants' partner was actually a research confederate and always the same person, a 22-year-old Japanese male. In order to control the participant's impression of the partner, the partner acted and talked exactly in the same way throughout all the experimental sessions.

Scales

Our previous trial showed the positive correlation between participants' scores in trust game and their pre-evaluation scores in others' trustworthiness, while we did not examined other psychological factors and thus the underlying mechanisms were not clarified [28]. Therefore, we examined the effects of anxiety and personality, in addition to the trust scores, in this trial. The following self-rated questionnaires were completed by the participants at pre- and post-treatment.

Temperament and Character Inventory (TCI)

TCI is based on the seven-factor model of temperament and character in personality [31]. According to TCI model, personality is classified into temperament, which consists of Novelty Seeking (NS), Harm Avoidance (HA), Reward Dependence (RD), Persistence (PS), and character, which consists of Self-Directedness (SD), Cooperativeness (C), Self-Transcendence (ST) with a four-point Likert type scale. We used a Japanese version with 125 questions (TCI-125) [32], which was kindly provided for use in this study from the HUMAN CAPITAL CONSULTING Corporation, Tokyo, Japan.

State-Trait Anxiety Inventory (STAI)

This anxiety scale with 20 questions consists of two factors; state anxiety, which refers to relatively unstable emotional threat to

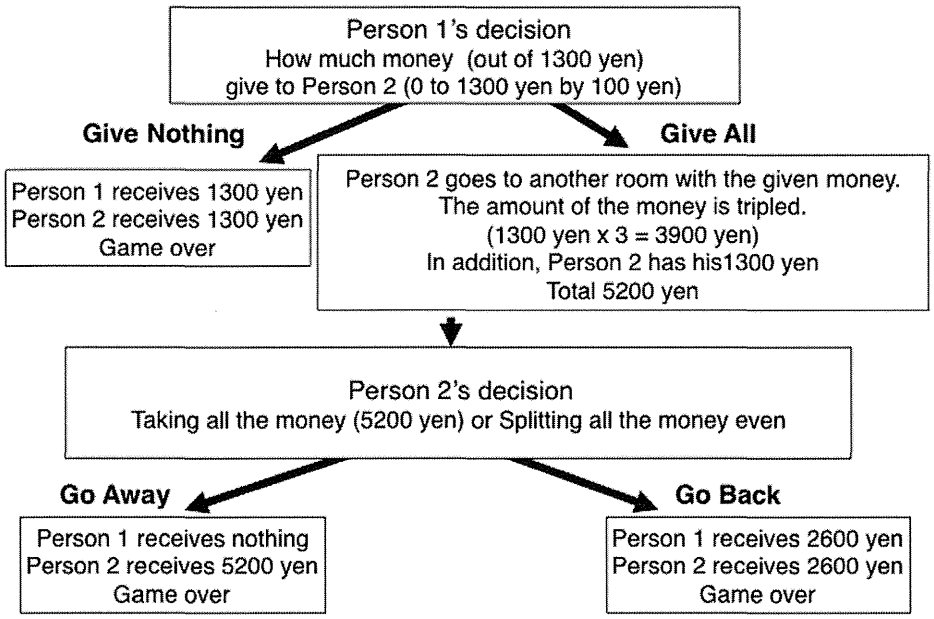

Figure 2. Trust Game Structure.
doi:10.1371/journal.pone.0040461.g002

current situations, and trait anxiety, which refers to relatively stable emotional threat consistently felt in daily life [33].

General Trust Scale (GTS)

GTS consists of six questions with a seven-point Likert type scale developed by Yamagishi and Yamagishi [34]. This scale measures respondents' estimation of others' trustworthiness. The reliability and validity of GTS have been confirmed across many countries [35]. According to past research on GTS, the major confounders of general trust are culture, sex and education level [34]. To eliminate the effects of these confounders, we recruited a homogenous sample as possible. As a result, all the participants were Japanese males and who had collage/university level educations so that we could test the effect of general trust without these confounders.

Data Analysis

Ninety-nine Japanese males, out of 101 entries, completed our experiments (mean age 21.52 years, SD 1.65 years), and analysis was conducted on this data. Among the participants, four (three in the minocycline condition, one in the control condition) failed to complete the questionnaires of STAI and GTS, so the analyses including these two scales were performed with the data of the 95 participants. All of the data analyses were performed with SPSS ver.19.

Results

In our previous trial, the statistical power was 0.766, and the statistical power in the present trial is 0.847. Therefore, the present trial exceeds the suggested efficient power of 0.8. The following analyses are shown with this more appropriate power.

Behavior in Trust Game

We compared the mean amount of participants' monetary offers in trust game by a t-test (**Table 1**). The monetary score in trust game was significantly lower in the minocycline group compared to the placebo group ($t(97) = 2.08$, $p<.05$). This result is consistent with our pilot study [28].

Effects of Minocycline on Personality, Anxiety and Trust

The effects of minocycline on personality, anxiety and trust were evaluated with the seven subscales of TCI, the two subscales of STAI, and GTS. We performed ANOVA with a repeated measure; the scores of the subscales as the dependent variable, and drug condition (Minocycline vs. Control), repeated measure of the subscales' scores (*Before* vs. *After* treatment) and their interaction as independent variables (**Table 1**).

There was no significant interaction term on each of the subscale of TCI. The main effect of time (*Before* vs. *After* treatment) was significant for *Persistence*. The score of *Persistence* is higher *After* (mean score = 13.09, SD = .237) than *Before* (mean score = 13.46, SD = .236). No effect was found on the rest of the items. These results indicate that participants' personality itself was not significantly affected by minocycline.

On STAI, interaction effect and main effect were significant on *Before-After* for state anxiety. Compared to the control group, the state anxiety score increased steeply in the minocycline group. According to simple main effect test, the score after the treatment was significantly higher in the minocycline group than in the control group ($p<.001$). Thus, this result may explain the cause of the lower trusting behavior for minocycline group in trust game. We found no significant effect on trait anxiety.

On GTS, there were no main or interaction effects.

Effects of Minocycline on Decision-Making Style

Next, to examine the effects of minocycline on decision-making style, we performed a multiple linear regression analysis of the amount of money offered (monetary score) in trust game as the dependent variable, and subscales of TCI, STAI and GTS as independent variables by conditions (**Table 2**). We revealed that state anxiety ($\beta = -.795$, $t = -4.42$, $p = .001$) and trust ($\beta = .321$, $t = 2.35$, $p = .023$) have significant effects in the minocycline group ($R^2 = .288$, $F(3,46) = 9.30$, $p = .001$) while only cooperation scale of

Table 1. Behavior in Trust Game, and Effects of Minocycline on Personality, Anxiety and Trust.

Category	Subcategory	Before Treatment		After Treatment		Before-After	Control-Minocycline	Interaciton
		Control	Minocycline	Control	Minocycline			
Monetary Score in Trust Game (%)	–	N/A	N/A	61.38 (32.43)	48.77 (27.70)	N/A	$t(97) = 2.08$, $p<.05$	N/A
TCI (from 1 to 20)	**Self-Transcendence**	10.69 (2.05)	10.82 (2.19)	10.52 (2.47)	10.57 (2.63)	*ns.*	*ns.*	*ns.*
	Cooperative-ness	14.98 (1.79)	14.98 (1.89)	14.80 (1.91)	14.79 (1.98)	*ns.*	*ns.*	*ns.*
	Self-Directedness	12.87 (0.20)	12.71 (0.22)	12.62 (1.98)	12.22 (2.09)	*ns.*	*ns.*	*ns.*
	Persistence	12.86 (2.14)	13.54 (2.53)	13.31 (2.34)	13.76 (2.25)	*ns.*	*ns.*	*ns.*
	Reward Dependence	14.07 (1.88)	14.28 (2.38)	14.10 (1.75)	14.10 (2.21)	*ns.*	*ns.*	*ns.*
	Harm Avoidance	13.51 (2.47)	13.30 (2.37)	13.55 (2.50)	13.26 (2.56)	*ns.*	*ns.*	*ns.*
	Novelty Seekng	12.97 (1.69)	12.99 (1.76)	12.94 (1.77)	13.02 (1.62)	*ns.*	*ns.*	*ns.*
STAI (from 1 to 4)	**State Anxiety**	2.04 (0.45)	2.00 (0.53)	2.11 (0.51)	2.28 (0.57)	$F(1, 93) = 18.60$ $p<.01$	*ns.*	$F(1, 93) = 6.57$ $p<.05$
	Trait Anxiety	2.33 (0.52)	2.21 (0.56)	2.27 (0.51)	2.27 (0.58)	*ns.*	ns.	ns.
General Trust Score (from 1 to 7)	-	4.31 (1.06)	4.51 (1.12)	4.41 (1.07)	4.53 (1.04)	*ns.*	*ns.*	*ns.*

We performed t-test on the behavior (monetary score) in trust game, and the average scores are shown in the Table. The effects of minocycline on personality, anxiety and trust were evaluated with the seven subscales of TCI, the two subscales of STAI, and GTS. We performed ANOVA with a repeated measure; the scores of the subscales as the dependent variable, and drug condition (Minocycline vs. Control), repeated measure of the subscales' scores (*Before* vs. *After* treatment) and their interaction as independent variables. As four participants (three for control, one for minocycline group) failed to complete the questions of STAI and GTS, 95 sets of data were analyzed. Significant and/or marginal effects are shown in the Table. Results were expressed as means (S.D.).

doi:10.1371/journal.pone.0040461.t001

TCI ($\beta = .486$, $t = 2.58$, $p = .013$) was significant in the control group ($R^2 = .092$, $F(3,42) = 2.51$, $p = .078$). Our novel finding in the present study is that the effect of state anxiety was stronger than that of trustworthiness. In sum, for the minocycline group, the less state anxiety and the more trustful, the more trusting behavior; while for the control group, the more cooperativeness, the more trusting behavior.

Discussion

As a first step to explore how microglia modulates human social/mental activities, we showed the novel effect of minocycline, the most famous inhibitor of microglial activation, on human monetary decision-making in trust game. Our previous trial, with smaller sample size and weaker statistical power, indicated the positive effect of minocycline on trust game, while the significant results were limited. In the present trial, we newly revealed that the monetary score in trust game was significantly lower in the minocycline group. Another novel finding was that minocycline treatment itself did not change personality, while, surprisingly participants' ways of decision-making were significantly shifted; cooperativeness, one component of personality, was the main modulating factor of decision-making in the placebo group, on the other hand, the minocycline group was mainly modulated by state anxiety and trustworthiness, both of which are known to be mainly dependent on real-time environments such as present social situation. In addition, the effect of state anxiety was stronger than that of trustworthiness. These results suggest that minocycline led to more situation-oriented decision-making, supporting our "noise reduction" hypothesis [28]; participants' personality may act as a "noise" during human social decision-making and minocycline may mimic personality- oriented behaviors.

Impact of Microglia on Personality-Oriented Social Behaviors

The novel effects of minocycline may explain the unknown role of microglia in social/mental activities. Until now, no study has reported microglial activities in healthy human subjects, while microglia have proved to play important roles in normal brain by communicating with neurons via releasing mediators and synaptic direct contact in rodent studies [14,15,16]. Therefore, human microglia may perform actively even in healthy brains, and inhibiting microglial activation with minocycline may create a shift from personality-oriented behaviors to situation-oriented behaviors by modulating neuro-synaptic-microglial networks. Rodent microglia play essential roles in synaptic pruning [18], which has pointed to the cryptic roles of microglia in human brain development. A recent study suggests that rodent microglial activation by infections during early developmental periods last, and these pre-activated microglia will be re-activated rapidly compared to normal state microglia [36]. Another study has suggested that microglia have a crucial role in the process of early-life memory in rats [37]. Early-life events can significantly modulate normal learning-dependent cytokine activity within the hippocampus, via a specific, enduring impact on brain microglial function, and preventing microglial activation by minocycline during learning prevents memory impairment in neonatally infected rats. Microglia are known to be activated not only by infection but also by physical and psychological stress in rodent studies [12,38,39,40]. In addition, Wei et al. reported that early life stress inhibits expression of a novel innate immune pathway in the developing hippocampus in pups [41]. Based on these recent findings, we suggest the possible existence of the following mechanism on personality and social behaviors; early-life environmental experiences such as psychological stress and traumatic events may activate human microglia, establish a certain neuro-synaptic-microglial connection, which may be memorized unconsciously as a primer for an extended period, and this formation in the human brain may determine each human's personality and personality- oriented social behaviors in later life (**Figure 3**). In addition, we can interpret the present results as follows; the control group's personality- oriented behaviors could be formulated by microglial priming effects, and the minocycline group's situation- oriented behaviors may be induced by suppressing microglial contribution to social behaviors. Further studies are needed to clarify contributions of microglia to human development including personality formation, and social/mental activities in later life.

Clinical Implication

Minocycline has been suggested to be an effective drug for psychiatric disorders [10,11]. Disturbed decision-making is a common symptom of various psychiatric disorders [42,43], and this disturbance is treated by psychotropic drugs such as antipsychotics and antidepressants, which have proved to inhibit microglial activation from *in vitro* studies [44,45,46,47,48]. In addition, a recent study suggests that effort-based decision-making in rat is modulated by estradiol [49], a sex hormone, which also has inhibitory effects on microglial activation [50,51]. These data support our minocycline results, and indicate that psychiatric

Table 2. Multiple Regression Analysis on Behavior in Trust Game.

Independent Variable	Control Group	Minocycline Group
	Beta	Beta
Cooperativeness (TCI)	.486*	
Reward Dependence(TCI)	−.281	
Self-Directedness (TCI)	−.284	
State Anxiety (STAI)		−.583**
General Trust		.321*
	$N = 46$, $R^2 = .092$, $F(3, 42) = 2.51$, $p < .10$	$N = 49$, $R^2 = .288$, $F(2, 46) = 9.30$, $p < .001$

Note: *p<.05,
**p<.01.
We performed a multiple linear regression analysis of the amount of money offered in trust game as the dependent variable, and subscales of TCI, STAI and GTS as independent variables by conditions. Remarkable effects are shown in the Table.
doi:10.1371/journal.pone.0040461.t002

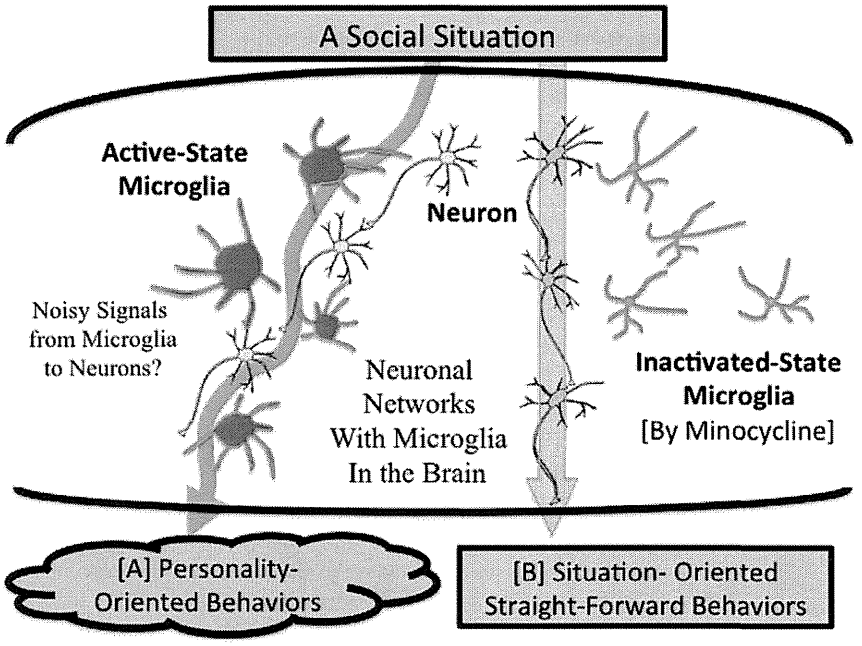

Figure 3. Possible Impact of Microglia on Personality and Social Behaviors. Early-life environmental experiences such as psychological stress and traumatic events may activate human microglia, establish a certain neuro-synaptic-microglial connection, which is memorized unconsciously as a primer for an extended period, and this formation in the human brain determines each human's personality and personality-oriented social behaviors in later life. In sum, neuronal networks with active microglia may induce noisy-decision-making, which is equivalent to personality- oriented behaviors (A). On the other hand, decision-making with neuronal dominant networks may induce straightforward behaviors, which are less affected by personality (B). In the present study, the control group's personality- oriented behaviors could be formulated by microglial priming effects (A), and the minocycline group's situation- oriented behaviors may be induced by suppressing microglial contribution to social behaviors (B).
doi:10.1371/journal.pone.0040461.g003

treatments may modulate microglial contribution to disturbed decision-making in social behaviors. To develop our results and these perspectives, animal based decision-making experiments with minocycline (or other microglial inhibitors) and histological analysis of microglia are called for in the near future. In addition, clinical trials of social decision-making experiments focusing on microglia should be attempted.

Limitation

First, this study did not examine the dose-dependent effects of minocycline. Second, this study was conducted only with adult males, while there may be a difference when players are female. Third, we did not measure microglia activity in the brain via imaging methods, while minocycline may inhibit some brain regional activities which are thought to be linked to trust and social decision-making [52,53]. Therefore, brain imaging studies are needed to clarify these regional activation mechanisms. Finally, other possible minocycline effects should be taken into account. Apart from inhibiting microglial activation, minocycline also has been reported to interact with brain glutamate and dopamine neurotransmission [54,55] and to have direct effects on neuronal cell line, PC12 [56]. Some reports suggest positive links between microglia, glutamate and dopamine interaction [57,58]. Further research should be performed to clarify this interaction mechanism. No specific inhibitor of microglia exists to date, therefore we selected minocycline as the most appropriate and safest drug to be used in humans at present. When a safe, specific inhibitor of microglial activation is developed, microglial human function will be clarified more effectively.

Conclusion

Based on the results of the present human social decision-making experiment, we have proposed a novel microglial contribution to personality and social behaviors. Our present study may shed new light on microglial roles in the social and mental life of healthy humans and also of people with psychiatric disorders. To explore these perspectives, further *in vitro/in vivo* studies and translational research are needed.

Ethics Statement

This double-blind randomized study was approved by the Kyushu University Ethical Committee under the administration of the UMIN clinical trial center (**UMIN000004803**). All participants gave written informed consent to participate after a complete description of the study.

Supporting Information

Table S1 Participants List.
(XLS)

Checklist S1 CONSORT Checklist.
(DOC)

Protocol S1 Trial Protocol.
(DOC)

Protocol S2 Japanese Version of Trial Protocol.
(DOC)

Acknowledgments

We thank Prof. Toshinori Kitamura for his kind advice in the usage of TCI. We thank Kaori Ishibashi, Lui Aoki, Fumika Hideshima, Hideki Horikawa, Yoshihiro Seki, Mina Sato-Kasai and Yusuke Yamauchi for their assistance, and are indebted to all our participants.

Author Contributions

Conceived and designed the experiments: TAK MW. Performed the experiments: TAK MW ST KI. Analyzed the data: MW. Contributed reagents/materials/analysis tools: TAK MW KH AM HU SK. Wrote the paper: TAK MW.

References

1. Graeber MB, Streit WJ (2010) Microglia: biology and pathology. Acta Neuropathol 119: 89–105.
2. Hanisch UK, Kettenmann H (2007) Microglia: active sensor and versatile effector cells in the normal and pathologic brain. Nat Neurosci 10: 1387–1394.
3. Ransohoff RM, Cardona AE (2010) The myeloid cells of the central nervous system parenchyma. Nature 468: 253–262.
4. Morgan JT, Chana G, Pardo CA, Achim C, Semendeferi K, et al. (2010) Microglial activation and increased microglial density observed in the dorsolateral prefrontal cortex in autism. Biol Psychiatry 68: 368–376.
5. Monji A, Kato T, Kanba S (2009) Cytokines and schizophrenia: Microglia hypothesis of schizophrenia. Psychiatry Clin Neurosci 63: 257–265.
6. van Berckel BN, Bossong MG, Boellaard R, Kloet R, Schuitemaker A, et al. (2008) Microglia activation in recent-onset schizophrenia: a quantitative (R)-[11C]PK11195 positron emission tomography study. Biol Psychiatry 64: 820–822.
7. Tikka T, Fiebich BL, Goldsteins G, Keinanen R, Koistinaho J (2001) Minocycline, a tetracycline derivative, is neuroprotective against excitotoxicity by inhibiting activation and proliferation of microglia. J Neurosci 21: 2580–2588.
8. Yong VW, Wells J, Giuliani F, Casha S, Power C, et al. (2004) The promise of minocycline in neurology. Lancet neurology 3: 744–751.
9. Lampl Y, Boaz M, Gilad R, Lorberboym M, Dabby R, et al. (2007) Minocycline treatment in acute stroke: an open-label, evaluator-blinded study. Neurology 69: 1404–1410.
10. Levkovitz Y, Mendlovich S, Riwkes S, Braw Y, Levkovitch-Verbin H, et al. (2010) A double-blind, randomized study of minocycline for the treatment of negative and cognitive symptoms in early-phase schizophrenia. J Clin Psychiatry 71: 138–149.
11. Miyaoka T, Yasukawa R, Yasuda H, Hayashida M, Inagaki T, et al. (2008) Minocycline as adjunctive therapy for schizophrenia: an open-label study. Clin Neuropharmacol 31: 287–292.
12. Hinwood M, Morandini J, Day TA, Walker FR (2012) Evidence that Microglia Mediate the Neurobiological Effects of Chronic Psychological Stress on the Medial Prefrontal Cortex. Cereb Cortex 22: 1442–1454.
13. Neigh GN, Karelina K, Glasper ER, Bowers SL, Zhang N, et al. (2009) Anxiety after cardiac arrest/cardiopulmonary resuscitation: exacerbated by stress and prevented by minocycline. Stroke 40: 3601–3607.
14. Ransohoff RM, Stevens B (2011) Neuroscience. How many cell types does it take to wire a brain? Science 333: 1391–1392.
15. Graeber MB (2010) Changing face of microglia. Science 330: 783–788.
16. Wake H, Moorhouse AJ, Jinno S, Kohsaka S, Nabekura J (2009) Resting microglia directly monitor the functional state of synapses in vivo and determine the fate of ischemic terminals. J Neurosci 29: 3974–3980.
17. Tremblay ME, Stevens B, Sierra A, Wake H, Bessis A, et al. (2011) The role of microglia in the healthy brain. J Neurosci 31: 16064–16069.
18. Paolicelli RC, Bolasco G, Pagani F, Maggi L, Scianni M, et al. (2011) Synaptic pruning by microglia is necessary for normal brain development. Science 333: 1456–1458.
19. Sofuoglu M, Mooney M, Kosten T, Waters A, Hashimoto K (2011) Minocycline attenuates subjective rewarding effects of dextroamphetamine in humans. Psychopharmacology 213: 61–68.
20. Crockett MJ, Clark L, Tabibnia G, Lieberman MD, Robbins TW (2008) Serotonin modulates behavioral reactions to unfairness. Science 320: 1739.
21. Berg J, Dickhaut J, McCabe K (1995) Trust, Reciprocity, and Social History. Games and Economic Behavior 10: 122–142.
22. King-Casas B, Sharp C, Lomax-Bream L, Lohrenz T, Fonagy P, et al. (2008) The rupture and repair of cooperation in borderline personality disorder. Science 321: 806–810.
23. Barraza JA, McCullough ME, Ahmadi S, Zak PJ (2011) Oxytocin infusion increases charitable donations regardless of monetary resources. Horm Behav 60: 148–151.
24. Kosfeld M, Heinrichs M, Zak PJ, Fischbacher U, Fehr E (2005) Oxytocin increases trust in humans. Nature 435: 673–676.
25. Zak PJ, Stanton AA, Ahmadi S (2007) Oxytocin increases generosity in humans. PLoS One 2: e1128.
26. Zhong S, Israel S, Shalev I, Xue H, Ebstein RP, et al. (2010) Dopamine D4 receptor gene associated with fairness preference in ultimatum game. PLoS One 5: e13765.
27. Rogers RD (2011) The roles of dopamine and serotonin in decision making: evidence from pharmacological experiments in humans. Neuropsychopharmacology 36: 114–132.
28. Watabe M, Kato TA, Monji A, Horikawa H, Kanba S (2012) Does minocycline, an antibiotic with inhibitory effects on microglial activation, sharpen a sense of trust in social interaction? Psychopharmacology 220: 551–557.
29. Vilares I, Dam G, Kording K (2011) Trust and reciprocity: are effort and money equivalent? PLoS One 6: e17113.
30. Jonas M, Cunha BA (1982) Minocycline. Ther Drug Monit 4: 137–145.
31. Cloninger RC (1994) The temperament and character inventory (TCI): A guide to its development and use. St. Louis, MO: Center for Psychobiology of Personality, Washington University.
32. Kijima N, Tanaka E, Suzuki N, Higuchi H, Kitamura T (2000) Reliability and validity of the Japanese version of the Temperament and Character Inventory. Psychol Rep 86: 1050–1058.
33. Spielberger CD, Gursuch RL, Lushene RE (1970) Manual for the State-Trait Anxiety Inventory (Self-evaluation Questionnaire). Palo Alto, CA: Consulting Psychologists Press.
34. Yamagishi T, Yamagishi M (1994) Trust and commitment in the United States and Japan. Motivation and Emotion 18: 9–66.
35. Gheorghiu MA, Vignoles VL, Smith PB (2009) Beyond the United States and Japan: Testing Yamagishi's Emancipation Theory of Trust across 31 Nation. Soc Psychol Q 72: 365–383.
36. Bilbo SD, Schwarz JM (2009) Early-life programming of later-life brain and behavior: a critical role for the immune system. Front Behav Neurosci 3: 14.
37. Williamson LL, Sholar PW, Mistry RS, Smith SH, Bilbo SD (2011) Microglia and memory: modulation by early-life infection. J Neurosci 31: 15511–15521.
38. Sugama S, Takenouchi T, Fujita M, Conti B, Hashimoto M (2009) Differential microglial activation between acute stress and lipopolysaccharide treatment. J Neuroimmunol 207: 24–31.
39. Schiavone S, Sorce S, Dubois-Dauphin M, Jaquet V, Colaianna M, et al. (2009) Involvement of NOX2 in the development of behavioral and pathologic alterations in isolated rats. Biol Psychiatry 66: 384–392.
40. Wohleb ES, Hanke ML, Corona AW, Powell ND, Stiner LM, et al. (2011) beta-Adrenergic receptor antagonism prevents anxiety-like behavior and microglial reactivity induced by repeated social defeat. J Neurosci 31: 6277–6288.
41. Wei L, Simen A, Mane S, Kaffman A (2012) Early life stress inhibits expression of a novel innate immune pathway in the developing hippocampus. Neuropsychopharmacology 37: 567–580.
42. Bjork JM, Momenan R, Hommer DW (2009) Delay discounting correlates with proportional lateral frontal cortex volumes. Biol Psychiatry 65: 710–713.
43. Loughland CM, Williams LM, Gordon E (2002) Schizophrenia and affective disorder show different visual scanning behavior for faces: a trait versus state-based distinction? Biol Psychiatry 52: 338–348.
44. Kato T, Mizoguchi Y, Monji A, Horikawa H, Suzuki SO, et al. (2008) Inhibitory effects of aripiprazole on interferon-gamma-induced microglial activation via intracellular Ca2+ regulation in vitro. J Neurochem 106: 815–825.
45. Kato T, Monji A, Hashioka S, Kanba S (2007) Risperidone significantly inhibits interferon-gamma-induced microglial activation in vitro. Schizophr Res 92: 108–115.
46. Horikawa H, Kato TA, Mizoguchi Y, Monji A, Seki Y, et al. (2010) Inhibitory effects of SSRIs on IFN-gamma induced microglial activation through the regulation of intracellular calcium. Prog Neuropsychopharmacol Biol Psychiatry 34: 1306–1316.
47. Kato TA, Monji A, Mizoguchi Y, Hashioka S, Horikawa H, et al. (2011) Anti-Inflammatory properties of antipsychotics via microglia modulations: are antipsychotics a 'fire extinguisher' in the brain of schizophrenia? Mini Rev Med Chem 11: 565–574.
48. Kato TA, Monji A, Yasukawa K, Mizoguchi Y, Horikawa H, et al. (2011) Aripiprazole inhibits superoxide generation from phorbol-myristate-acetate (PMA)-stimulated microglia in vitro: implication for antioxidative psychotropic actions via microglia. Schizophr Res 129: 172–182.
49. Uban KA, Rummel J, Floresco SB, Galea LA (2012) Estradiol modulates effort-based decision making in female rats. Neuropsychopharmacology 37: 390–401.
50. Akabori H, Moeinpour F, Bland KI, Chaudry IH (2010) Mechanism of the anti-inflammatory effect Of 17beta-estradiol on brain following trauma-hemorrhage. Shock 33: 43–48.
51. Saijo K, Collier JG, Li AC, Katzenellenbogen JA, Glass CK (2011) An ADIOL-ERbeta-CtBP transrepression pathway negatively regulates microglia-mediated inflammation. Cell 145: 584–595.
52. Lee D (2008) Game theory and neural basis of social decision making. Nat Neurosci 11: 404–409.
53. Converse AK, Larsen EC, Engle JW, Barnhart TE, Nickles RJ, et al. (2011) 11C-(R)-PK11195 PET imaging of microglial activation and response to minocycline in zymosan-treated rats. J Nucl Med 52: 257–262.
54. Yrjanheikki J, Tikka T, Keinanen R, Goldsteins G, Chan PH, et al. (1999) A tetracycline derivative, minocycline, reduces inflammation and protects against focal cerebral ischemia with a wide therapeutic window. Proc Natl Acad Sci U S A 96: 13496–13500.

55. Du Y, Ma Z, Lin S, Dodel RC, Gao F, et al. (2001) Minocycline prevents nigrostriatal dopaminergic neurodegeneration in the MPTP model of Parkinson's disease. Proc Natl Acad Sci U S A 98: 14669–14674.
56. Hashimoto K, Ishima T (2010) A novel target of action of minocycline in NGF-induced neurite outgrowth in PC12 cells: translation initiation [corrected] factor eIF4AI. PLoS One 5: e15430.
57. Tikka TM, Koistinaho JE (2001) Minocycline provides neuroprotection against N-methyl-D-aspartate neurotoxicity by inhibiting microglia. J Immunol 166: 7527–7533.
58. Purisai MG, McCormack AL, Cumine S, Li J, Isla MZ, et al. (2007) Microglial activation as a priming event leading to paraquat-induced dopaminergic cell degeneration. Neurobiol Dis 25: 392–400.

Published online 16 August 2012

Nucleic Acids Research, 2012, Vol. 40, No. 19 ***9717–9737***
doi:10.1093/nar/gks774

p32/gC1qR is indispensable for fetal development and mitochondrial translation: importance of its RNA-binding ability

Mikako Yagi[1], Takeshi Uchiumi[1,*], Shinya Takazaki[1], Bungo Okuno[1], Masatoshi Nomura[2], Shin-ichi Yoshida[3], Tomotake Kanki[1] and Dongchon Kang[1,*]

[1]Department of Clinical Chemistry and Laboratory Medicine, [2]Department of Medicine and Bioregulatory Science and [3]Department of Bacteriology, Graduate School of Medical Sciences, Kyushu University, 3-1-1 Maidashi, Higashi-ku, Fukuoka 812-8582, Japan

Received March 21, 2012; Revised July 23, 2012; Accepted July 24, 2012

ABSTRACT

p32 is an evolutionarily conserved and ubiquitously expressed multifunctional protein. Although p32 exists at diverse intra and extracellular sites, it is predominantly localized to the mitochondrial matrix near the nucleoid associated with mitochondrial transcription factor A. Nonetheless, its function in the matrix is poorly understood. Here, we determined p32 function via generation of p32-knockout mice. p32-deficient mice exhibited mid-gestation lethality associated with a severe developmental defect of the embryo. Primary embryonic fibroblasts isolated from p32-knockout embryos showed severe dysfunction of the mitochondrial respiratory chain, because of severely impaired mitochondrial protein synthesis. Recombinant p32 binds RNA, not DNA, and endogenous p32 interacts with all mitochondrial messenger RNA species *in vivo*. The RNA-binding ability of p32 is well correlated with the mitochondrial translation. Co-immunoprecipitation revealed the close association of p32 with the mitoribosome. We propose that p32 is required for functional mitoribosome formation to synthesize proteins within mitochondria.

INTRODUCTION

Mitochondria are essential organelles that are present in virtually all eukaryotic cells. The primary function of mitochondria is ATP production via the oxidative phosphorylation (OXPHOS) pathway. Additionally, mitochondria perform crucial roles in many other metabolic, regulatory and developmental processes. The circular 16.5-kb human mitochondrial DNA (mtDNA) molecule encodes 2 rRNAs, 22 tRNAs and 13 proteins that are members of the respiratory chain (1–3). All other proteins, including the mitochondrial translation apparatus, are derived from nuclear genes and are imported from the cytoplasm. In addition to core components of the small and large subunits of mitochondrial ribosomes (mitoribosomes), many other factors are required for translation initiation, elongation and termination in mitochondria (4).

Mammalian cells contain up to thousands of copies of mtDNA, which are organized in nucleoids (5,6). Mitochondrial transcription factor A (TFAM) is a key activator of mitochondrial transcription, and is a participant in mitochondrial genome replication to maintain mtDNA (7). It may also be a primary factor for packaging mtDNA in the nucleoid (8). Nucleoids may dynamically change their structure and distribution within mitochondria that are undergoing fission and fusion and are involved in various dynamic processes including mitochondrial replication, transcription and translation (9). Previously, we isolated p32 as a protein associated with TFAM (10).

Transcription from both the heavy-strand promoter (HSP) and light-strand promoter (LSP) generates polycistronic molecules that almost cover the entire H- and L-strand, respectively. It is generally accepted that tRNAs are excised from long polycistronic primary transcripts to generate mature messenger RNAs (mRNAs) and ribosomal RNAs (rRNAs); this is called the tRNA punctuation model (11–13). During or immediately after

*To whom correspondence should be addressed. Tel: +81 92 642 5750; Fax: +81 92 642 5772; Email: uchiumi@cclm.med.kyushu-u.ac.jp
Correspondence may also be addressed to Dongchon Kang. Tel: +81 92 642 5748; Fax: +81 92 642 5772; Email: kang@cclm.med.kyushu-u.ac.jp

The authors wish it to be known that, in their opinion, the first two authors should be regarded as joint First Authors.

cleavage of tRNAs, mRNAs are polyadenylated by a mitochondrial poly(A) polymerase. Indeed, in the case of some mRNAs, poly(A) tail addition is necessary to form a stop codon at the end of the open reading frame and may also be necessary for stabilization of some RNAs (14–16). Thus, nine monocistronic and two dicistronic mRNA transcripts are formed. Mitochondrial mRNAs do not contain 5′-modifications (13), and to date there has been no report of a canonical mitochondrial poly(A)-binding protein. Bioinformatic analyses revealed no obvious candidate, although several metabolic mitochondrial enzymes have been shown to be capable of binding RNA and poly(A) sequences (17,18). Another important post-transcriptional process is mRNA transfer to the mitoribosome, which is required to control RNA levels and translational activity. However, the proteins involved and the exact mechanism are yet to be revealed.

Protein–RNA interactions play essential roles in post-transcriptional control of gene expression including splicing, nuclear-cytoplasmic transport, localization, quality control, mRNA degradation and translational regulation (19). Numerous mitochondrial RNA-binding proteins without known RNA-binding domains have also been identified (18). AUH (AU RNA-binding protein /enoyl-CoA hydratase), which forms a doughnut-like structure composed of two trimers, is highly positively charged because of lysine residues in its α-helix H1 that is located on the edge of the cleft between the trimers. A mutational analysis showed that the lysine residues in the α-helix H1 are essential for the RNA-binding activity of AUH (20,21).

p32 [complement component 1, q subcomponent-binding protein (C1qBP); also called gC1qR or HABP1] was first isolated from a membrane preparation of Raji cells and originally copurified with the pre-mRNA splicing factor SRSF1 (also called SF2 and ASF) in human HeLa cells (22). The p32 protein is a doughnut-shaped trimer, which primarily localizes to the mitochondrial matrix, but has also been reported to be present at the cell surface, in the nucleus and cytosol, as well as within secretory granules (23–26). p32 is synthesized as a pre protein and is processed by proteolytic cleavage of the N-terminal amino acids containing the mitochondrial signal sequence (27). The pre-protein form of p32 is only expressed in germ cells (28), which clearly justifies the predominant localization of p32 in the mitochondrial matrix.

Human p32 interacts with various molecules including hyaluronic acids, human immunodeficiency virus Tat protein, complement 1q, proapoptotic factor HRK and tumor suppressor ARF (29–31). These observations suggest that p32 may be a multifunctional chaperone protein (32). HABP1/p32/C1qBP represented as, synonym in Human Genome, exhibits structural plasticity influenced by ionic environment due to asymmetric charge distribution. The presence of salt stabilizes the compact trimeric conformation and can interact with hyaluronan only (33). Thus, one of the ligand of this protein is hyaluronan, a complex mucopolysaccharide which is well known for its regulatory role during embryonic development (34). p32/HABP1 expression in *Schizosaccharomyces pombe* induces growth inhibition and morphological abnormalities such as elongation, multinucleation and aberrant cell septum formation in several strains, implying a role for this protein in cell-cycle progression and cytokinesis (35). However, the primary physiological role of p32 in mammalian cells is unclear, particularly in the mitochondrial matrix, despite its predominant localization there.

Previously, we identified a *Saccharomyces cerevisiae* homolog of human p32, mam33, which localized to the mitochondrial matrix. Mam33-deficient yeast cells are significantly defective in maintenance of the mitochondrial genome and show impairment of mitochondrial ATP synthesis. The growth impairment is restored by the introduction of human *p32* cDNA, which demonstrates the evolutionarily conserved function of p32 homologs among eukaryotes. Taken together, we propose that both human p32 and yeast mam33 reside in the mitochondrial matrix and play an important role in maintaining mitochondrial OXPHOS (27). Very recently, p32-knockdown cells exhibited reduced synthesis of mtDNA-encoded OXPHOS polypeptides and were less tumorigenic *in vivo* (36).

To explore the role of the p32 protein *in vivo*, particularly in the mitochondrial matrix, we generated mice with a homozygous disruption of the *p32* gene. We show that p32 inactivation causes mid-gestation lethality of knockout embryos and defects in OXPHOS, because of severe impaired protein synthesis of mtDNA-encoded protein. Here, we propose that the mitochondrial matrix protein p32 functions as an essential RNA-binding factor in mitochondrial translation, and is indispensable for embryonic development.

MATERIALS AND METHODS

Animals

Animals were mated overnight, and females were examined for a vaginal plug the following morning. At noon of that day, vaginal plug detection was recorded as embryonic day (E) 0.5. Mouse experiments were performed in accordance with the guidelines of the animal ethics committee of Kyushu University Graduate School of Medicine, Japan.

Immunoblotting

Briefly, cells were lysed with lysis buffer (50 mM Tris–HCl, pH 7.5, 1 mM EDTA, 150 mM NaCl and 0.5% NP-40) and then subjected to immunoblotting as described elsewhere (37). Signals were visualized with horseradish peroxidase (HRP)-conjugated anti-rabbit IgG and an enhanced chemiluminescence reagent (GE Healthcare, Piscataway, NJ). Chemiluminescence was recorded and quantified with a chilled charge-coupled device camera (LAS1000plus).

Immunofluorescence imaging of mouse embryonic fibroblasts

Immunofluorescence was carried out according to established techniques. Briefly, mouse embryonic fibroblasts

(MEFs) were incubated in the presence of 500 nM MitoTracker Red (Invitrogen) for 20 min. Cells were fixed and permeabilized, then incubated with a 1:200 dilution of anti-p32 serum in PBS/1% bovine serum albumin (BSA) for 1 h. Glass slides were mounted using Superfrost (Matsunami). Fluorescence images were obtained using a confocal laser microscope (Nikon).

Antibodies

Polyclonal antibodies against mouse p32, HA, TFAM, LRPPRC and VDAC were raised in our laboratory. Antibodies against COXI, COXIII, NDUFA9, SDHA, UQCRFS1, ATP synthase and COXVa were purchased from Invitrogen. Antibodies against β-actin, MRPS22, MRPS29 and MRPL3 were purchased from Sigma, Proteintech Group Inc, BD Biosciences and Abcam, respectively. Alexa 488-conjugated anti-rabbit and anti-mouse IgG for fluorescence microscopy, Alexa 568-conjugated anti-mouse IgG for fluorescence microscopy of paraffin-embedded tissue sections, HRP-conjugated anti-mouse IgG and diaminobenzidine (DAB) for BrdU staining were all purchased from Nichirei.

MEF culture and cell proliferation assay

SV40 large T antigen-immortalized MEFs were generated from E14 p32flox/flox C57BL/6 embryos by standard methods. MEFs and HeLa cell were cultured in Dulbecco's modified Eagle's medium (DMEM) (1000 mg/l glucose) supplemented with 10% FBS at 37°C in a humidified atmosphere with 5% CO_2. For cell proliferation assay, MEF cells (1×10^4) were seeded in triplicate in 35 mm dishes and cultured in DMEM (1000 mg/l glucose) plus dialyzed 10% fetal bovine serum (FBS) without pyruvate. Cells were trypsinized and counted daily for up to 96 h using a Coulter Counter (Beckman Coulter). Pyruvate (1 mM), uridine (0.2 mM) and glucose (3500 mg/l) were added on Days 0 and 4. We used dialyzed FBS to remove small molecules such as uridine and pyruvate.

RNA band-shift assays

RNA electrophoretic mobility shift assays (REMSAs) were carried out according to established techniques. Briefly, a synthesized oligonucleotide probe (DNA or RNA) was end-labeling in the presence of [γ-^{32}P]ATP by a T4 polynucleotide kinase. To form RNA–protein complexes, the indicated amount of purified His-p32 was incubated with the ^{32}P-labeled oligonucleotide probe at 25°C for 30 min in binding buffer [10 mM HEPES, pH 7.6, 3 mM $MgCl_2$, 20 mM KCl, 1 mM dithiothreitol (DTT), 50 U RNase inhibitor (Toyobo) and 5% glycerol]. Heparin (5 μg) was added for a further 10 min incubation to prevent non-specific binding. Samples were electrophoresed in a 6% non-denaturing polyacrylamide gel in Tris–borate buffer. Gels were dried and visualized using a BAS2500 (Fuji).

Sucrose gradient analysis of mitochondrial ribosomes

MEFs were solubilized in a non-ionic detergent (1% lauryl maltoside). Total cell lysates (2 mg) were loaded onto a 15–30% sucrose density gradient in 20 mM Tris–HCl, pH 7.5, 150 mM NaCl and 1 mM $CaCl_2$, and then centrifuged at 100 000*g* for 3 h at 4°C in a swinging bucket rotor (SW 40.1; Beckman Coulter). After separation, 17 fractions were precipitated by 10% trichloroacetic acid and washed in acetone, and then the entire fraction was resolved by SDS–polyacrylamide gel electrophoresis (PAGE).

ATP quantification

Cellular ATP was quantified using an ATP-determination kit according to the manufacturer's instructions (Promega). Briefly, four MEFs, plated at equal densities, were lysed in passive lysis buffer (Promega). Equal volumes of cell lysate were added to the standard reaction solution, and luminescence was measured and normalized to the protein amount in each lysate. The values used were in the linear range of the assay as determined by a standard curve.

Oxygen consumption assay

Oxygen consumption was measured as described elsewhere (38). MEFs were trypsinized, PBS washed twice and then permeabilized with 0.1 μg/ml digitonin. The optimum incubation time for permeabilization (50 s for MEFs) was determined for each cell line as the shortest time after which 99% of cells were trypan blue-positive. Cells were placed into the reaction chamber of a Clark-type electrode (Hansatech), and oxygen concentrations were measured in 1 ml volumes at 37°C with substrates (glutamate + malate, succinate + glycerol-3-phosphate; Sigma) and inhibitors according to standard protocols (39). Oxygen consumption was represented as the mean ± SD, nanomoles O_2 consumed per minute per cell.

Expression constructs

The expression construct containing mouse p32 cDNA was generated by standard methods. Site-directed mutagenesis to generate p32 mutants K89A and K93A was performed using methods described elsewhere (37). cDNAs of wild-type and mutant K89A/K93A p32 were cloned into the BamHI/XhoI sites of the expression vector pcDNA3 (Invitrogen).

Immunoprecipitation using anti-HA antibodies

Immunoprecipitation (IP) was carried out according to established techniques (37). Doxycycline-induced and non-induced HeLa (p32-HA) cells (1×10^8 cells) and MEF cells were homogenized and centrifuged at 900*g* for 10 min. The supernatant (adjusted to 10% Percoll) was overlaid on a discontinuous Percoll density gradient (4 ml of 40% and 4 ml of 20% Percoll buffer; GE Healthcare) in a 12 ml centrifugation tube. After centrifugation at 60 000*g* for 1 h using a SW41-Ti rotor (Beckman Coulter), the mitochondrial phase located in the middle of the tube was collected. Two to three milligrams of

mitochondrial protein were solubilized in 1 ml IP buffer (10 mM Tris–HCl, pH 7.4, 150 mM NaCl, 1 mM EDTA, 1% NP-40 and 0.1% SDS) containing 40 µl of beads coated with anti-HA or anti-p32 antibody. After 12 h of rotation, the beads were washed four times with IP buffer and eluted with 0.1 M glycine (pH 2.5).

Pulse-labeling of mitochondrial translation products

Mitochondrial translation products were pulse-labeled *in vitro* with [^{35}S]-(methionine and cysteine) (GE Healthcare). In experiments where the label was chased, cells were incubated for 6 min in 100 µg/ml emetine or 250 µg/ml chloramphenicol prior to labeling for 60 min. Labeled cells were then rinsed with an Hypotonic buffer (10 mM Tris–HCl, pH 7.4, 150 mM $MgCl_2$, 10 mM KCl). After centrifugation at 1150*g* for 5 min, cell pellets were resuspended in loading buffer consisting of 93 mM Tris–HCl, pH 6.7, 7.5% glycerol, 1% SDS, 0.25 mg/ml bromophenol blue and 3% mercaptoethanol. The total lysate was then subjected to 15% SDS-PAGE for 3 h at 180 V. Gels were measured using a BAS2500 (Fuji).

RNA co-IP with p32-HA protein

Briefly, HeLa whole cell lysates induced by doxycycline were first precleared with 50 µg rabbit IgG (Bio-Rad) for 15 min at 4°C, followed by binding to anti-HA-coated agarose beads or anti-LRPPRC antibody with protein G agarose for 12 h at 4°C. Then, p32-HA was eluted using glycine (pH 2.5), and RNA was extracted with an RNAeasy kit (Qiagen). The eluted RNA was treated with 100 U DNase I at 37°C for 20 min, and then the RNA was purified again with an RNAeasy kit.

Activity of respiratory mitochondrial complex

MEFs were lysed in a hypotonic buffer (2.5 mM Tris–HCl, pH 7.5 and 2.5 mM $MgCl_2$) on ice for 15 min, and then sonicated for 15 s (25% output, duty cycle; TAITEC) to measure respiratory complex activity.

To detect complex I activity, spectrophotometric assays were performed to evaluate NADH:Q oxidoreductase activity at 30°C by monitoring the decrease in the absorbance of nicotinamide adenine dinucleotide reduced form (NADH) at 340 nm, as described elsewhere (40). Briefly, 10 µM decylubiquinone (artificial electron acceptor), 2 µg antimycin A (complex III inhibitor), 5 mM sodium azide (NaN_3) (complex IV inhibitor) and 0.5 mg whole-cell lysate were mixed in 1 ml standard reaction medium (2.5 mM $MgCl_2$ and 50 mM inorganic phosphate, pH 7.3). The reaction was initiated with 100 µM NADH. The activity of the enzyme was determined by the difference of absorbance with and without 1.25 µg rotenone (complex I inhibitor). Data were expressed as nmol NADH oxidized/min/µg protein.

Succinate dehydrogenase (complex II) activity was determined spectrophotometrically at 30°C (41). Briefly, the reaction was initiated with 50 µM dichlorophenolindophenol (DCPIP; used as an artificial electron acceptor) in 1 ml standard reaction medium supplemented with 20 mM succinate, 2 µg rotenone, 2 µg antimycin A, 5 mM NaN_3 and 0.1 mg whole-cell lysate.

Cytochrome c reductase (complex III) activity was evaluated spectrophotometrically at 30°C by monitoring the increase in absorbance at 550 nm of cytochrome c. Briefly, the reaction was initiated by the addition of 5 mM reduced decylubiquinone to 1 ml standard reaction medium supplemented with 2 µg rotenone, 5 mM NaN, 60 µM cytochrome c and cell lysate. The reaction was stopped by addition of 2 µg Antimycin A.

Cytochrome c oxidase (complex IV) activity was determined spectrophotometrically at 550 nm at 30°C (42). Briefly, the reaction was initiated by the addition of 50 µg whole-cell lysate to 1 ml standard reaction medium supplemented with 20 µM ferrocytochrome c.

mRNA quantification

RT of 1 µg total RNA was performed with random hexamer primers using SuperScript II RT (Invitrogen) according to the manufacturer's instructions. The expression of mitochondrial genes was detected by qPCR with a thermal cycler (StepOne plus; Applied Biosystems). PCR primers are listed in Supplementary Table S1.

Measurement of mitochondrial membrane potential

Mitochondrial membrane potential ($\Delta\psi m$) was estimated using a JC-1 probe (Invitrogen). This reagent is a highly reliable, cationic and mitochondria-specific fluorescent dye, which becomes concentrated in mitochondria in proportion to the membrane potential, because it is highly lipophilic. Increasing amounts of dye accumulate in mitochondria with increasing $\Delta\psi m$ and ATP-generating capacity. The dye is present as monomers at lower concentrations (green fluorescence), but at higher concentrations forms J-aggregates (red fluorescence). The ratio of the fluorescence at 590 nm to that at 527 nm represents the relative $\Delta\psi m$ value. Fluorescence was measured at the two wavelengths by a FACS Caliber (Becton Dickinson).

RESULTS

Disruption of *p32* causes embryonic lethality

To experimentally address the function of p32 in a physiological *in vivo* context, we used gene targeting to generate p32-deficient mice. We constructed a gene replacement vector that introduced a gene cassette, consisting of the neomycin resistance gene (*Neo*) and flanking *loxP* sites upstream and downstream of exon 3, into the endogenous *p32* gene (Supplementary Figure S1A). After injection of embryonic stem cells harboring the targeted allele, germline transmission was confirmed by Southern blotting and PCR analysis (Supplementary Figure S1B and S1C). Heterozygous $p32^{+/-}$ mice were generated by breeding $p32^{fl/+}$ mice with a *Cre* transgenic mouse strain (EII-Cre) allowing universal expression of Cre-recombinase in all tissues. Intercrosses of $p32^{+/-}$ mice revealed no viable $p32^{-/-}$ offspring (Supplementary Figure S1D and Table 1). To determine the time at which the p32 mutant became lethal, we examined embryos from $p32^{+/-}$ intercrosses at various developmental stages. In contrast to wild-type embryos, the growth of

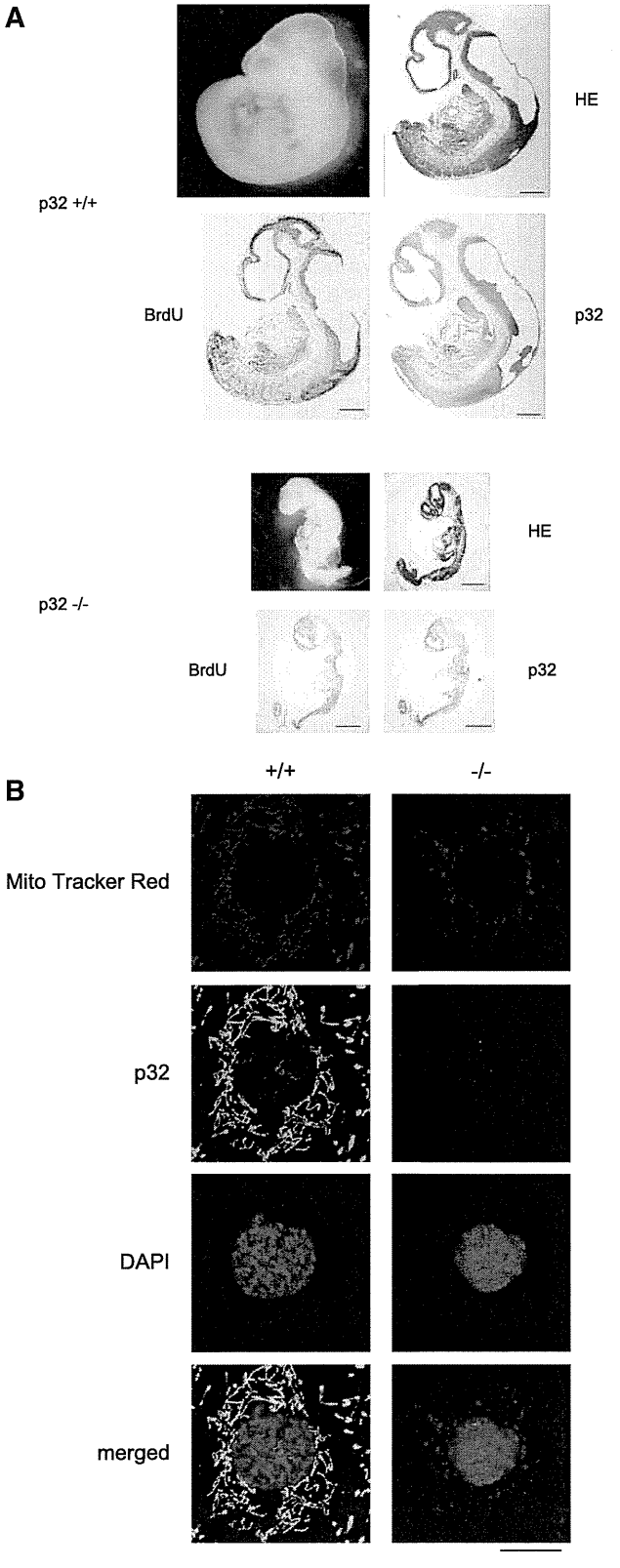

Figure 1. Disruption of p32 causes embryonic lethality. (**A**) Whole mounts of E10.5 $p32^{-/-}$ embryos and histological analysis of $p32^{-/-}$ embryos compared with those of wild-type $p32^{+/+}$ littermates. Photomicrographs (upper left) and hematoxylin and eosin (HE) staining (upper right) are shown. Pregnant mice were injected with BrdU at 2 h prior to dissection. Sections of $p32^{+/+}$ and $p32^{-/-}$ embryos at E10.5 were stained with BrdU (lower left) or an anti-p32 antibody (lower right). *In vivo* labeling with BrdU revealed arrest of proliferation in E10.5 embryos. Scale bars: 500 μm. (**B**) Immunofluorescence staining of p32 and MitoTracker Red in wild-type and p32-knockout cells. Nuclei were stained with 4′,6-diamidino-2-phenylindole (DAPI). MEFs were treated with MitoTracker Red (500 nM) for 20 min before p32 staining. Cells were fixed, fluorescently stained by anti-p32 antibodies, and then analyzed by confocal microscopy. The lower panel shows merged images. Scale bar: 20 μm.

Table 1. p32 deficiency causes embryonic lethality

	Genotype			Disintegrated or resorbed	Total
	+/+	+/−	−/−		
E8.5	8	19	5	5	32
E9.5	17	35	15	17	67
E10.5	5	16	7	10	28
E11.5	4	15	6	4	25
E12.5	1	9	2	3	12
E13.5	3	21	1	2	25
Newborn	21	41	0		62

Embryos at the indicated stages were isolated from intercrosses of heterozygous mice, and the total numbers (*n*) of intact and disintegrated or resorbed embryos were counted.

$p32^{-/-}$ embryos appeared retarded as early as E10.5. Most $p32^{-/-}$ embryos had been resorbed by E11.5, and therefore $p32^{-/-}$ embryos died between E10.5 and E11.5.

The phenotype of $p32^{-/-}$ embryos included markedly shrunken, poorly developed, pale and anemic organs (Figure 1A). p32 protein was absent from $p32^{-/-}$ embryos. In E10.5 $p32^{-/-}$ embryos, BrdU incorporation revealed that cells did not proliferate in various tissues including the brain, heart and liver. These data suggest that growth retardation, smaller size of organ and severe anemia account for the embryonic lethality of the p32 mutation.

Establishment of p32-knockout MEFs

To define the functional consequences of *p32* deletion, MEFs were isolated from homozygous $p32^{flox/flox}$ embryos and infected with a adenovirus encoding Cre-recombinase, which led to efficient deletion of p32 *in vitro*. We also immortalized $p32^{-/-}$ cells by transfection with a plasmid vector encoding the SV40 large T antigen. Western blot analysis confirmed the absence of p32 in $p32^{-/-}$ cells and half wild-type p32 levels in $p32^{+/-}$ cells (Supplementary Figure S2). $p32^{-/-}$ MEFs exhibited an enlarged and flattened cell morphology compared with that of $p32^{+/+}$ MEFs, suggesting that loss of p32-induced cell morphological change.

Abnormal mitochondrial morphology in $p32^{-/-}$ MEFs

Maintenance of proper mitochondrial morphology is critical for the function of this organelle. The basic morphology of mitochondria in cells is a dynamic tubulovesicular reticulum. Mitochondrial morphology changes dynamically as a result of a balance in the fusion and fission occurring in response to cellular energy demands, differentiation and pathological conditions (43,44). Therefore, we determined the effect of p32 depletion on the morphology of mitochondria using

Mitotracker Red in $p32^{+/+}$ and $p32^{-/-}$ MEF cell lines. In wild-type cells, p32 colocalized to the tubulovesicular mitochondria. In contrast, upon loss of p32, the tubular mitochondrial organization shifted to a punctate, granular shape (Figure 1B). This result suggests that the loss of p32 exhibited tubulovesicular morphological change.

Establishment of mitochondrial re-expression of p32

To directly confirm that p32 regulated mitochondrial function, we expressed mitochondria-targeted and cytoplasmic forms of p32 in $p32^{-/-}$ MEFs. We obtained stable $p32^{-/-}$ MEFs that expressed a low level of mitochondrially targeted p32 (immature) (Supplementary Figure S3A). The recombinant p32 was the same size as endogenous p32, suggesting that we successfully restored p32 expression in knockout cells, albeit at low levels. The cDNA construct encoded a p32 protein lacking the first 71 amino acids, which produced a cytoplasm-only p32. The expression level of this cytoplasm-only p32 was significantly lower than that of the mitochondria-targeted p32 (Supplementary Figure S3B). We were able to observe the cytoplasmic p32 only after inhibition of proteasomal degradation with MG-132 (Supplementary Figure S3C). These data suggest that cytoplasmic p32, which is unable to localize to the mitochondria, is extremely unstable in MEFs.

Loss of p32 reduced complex activity

We first sought to investigate a possible role for p32 in OXPHOS. The electron transport chain consists of five multi-subunit enzymatic complexes formed from the products of both nuclear and mitochondrial genes. We measured the activities of the electron transport chain complexes by spectroscopic assays that revealed the activities of complexes I, III and IV were strongly reduced in $p32^{-/-}$ cells, while the activity of complex II was unchanged (Figure 2A). Interestingly, complex II is the only OXPHOS complex encoded exclusively by nuclear DNA. Re-expression of p32 in $p32^{-/-}$ cells partially restored complex I, III and IV activities. These finding suggested that p32 might be involved in mtDNA-related protein function because complexes I, III and IV include proteins encoded by mtDNA.

Mammalian p32 is required for oxidative respiration

To further test mitochondrial OXPHOS function, we measured cellular respiration by polarographic assays of digitonin-permeabilized cells. Oxygen electrode studies showed a 3-fold decrease in oxygen consumption dependent on complexes I + III + IV (glutamate + malate) and complexes III + IV (succinate + G3P) in p32-knockout MEFs compared with those of wild-type MEFs (Figure 2B), indicating that p32 is required for mitochondrial respiration. Decreased respiration in p32-knockout MEFs suggests a reduction in functional respiratory complexes.

p32-knockout MEFs show reduced mitochondrial membrane potential and ATP production

We suspected that p32-mediated inhibition of the mitochondrial respiratory chain may affect the mitochondrial membrane potential ($\Delta\psi m$). The $\Delta\psi m$ value was measured using JC-1, a fluorescent dye sensitive to mitochondrial membrane potential. The $\Delta\psi m$ values of p32-knockout MEFs were lower than those of wild-type MEFs (Figure 2C). Carbonyl cyanide 3-chlorophenylhydrazone (CCCP)-treated cells served as a positive control for depolarization of the mitochondrial membrane.

Because mitochondria are the cellular powerhouses for energy production, we measured ATP levels in wild-type and $p32^{-/-}$ MEFs. In wild-type cells, the inhibition of glycolysis by 2-deoxy-glucose (2DG) only slightly decreased the ATP level (Figure 2D, upper set, $p32^{+/+}$, lane 2) probably because pyruvate in DMEM supported mitochondrial OXPHOS. After oligomycin, an inhibitor of complex V, was added together with 2DG, the cellular ATP level was strongly decreased (Figure 2D, upper set, $p32^{+/+}$, lane 3), indicating that wild-type MEFs were largely dependent on mitochondrial ATP production (see lower set and legends for calculation). The total ATP level was rather higher in p32-knockout MEFs than in wild-type MEFs (Figure 2D, upper set, $p32^{+/+}$, lane 1 and $p32^{-/-}$, lane 1). A marked decrease in mitochondrial ATP production by 2DG was observed in the knockout MEFs (upper set, $p32^{-/-}$, lane 2) and further addition of oligomycin marginally decreased the ATP production (upper set, $p32^{-/-}$, lane 3), indicating that p32-knockout MEFs mostly depends on glycolytic ATP production. The decrease in mitochondrial ATP production may be over-compensated by glycolytic ATP production that was estimated by 2DG-sensitive cellular ATP (Figure 2D, lower set table). Re-expression of p32 in $p32^{-/-}$ cells restored mitochondrial ATP production, but not the introduction of an empty vector, indicating that p32 is required for efficient ATP production via OXPHOS.

Retarded proliferation of $p32^{-/-}$ MEFs

To assess potential defects in proliferation caused by mitochondrial OXPHOS dysfunction, we cultured cells at a standard concentration of glucose (1000 mg/l) without pyruvate, which allowed easier observation of the effects of glucose on OXPHOS. We dialyzed FBS to remove small molecules such as uridine and pyruvate. As shown in Figure 2E, proliferation of p32-knockout MEFs was strongly retarded compared with that of wild-type cells. Re-expression of p32 in $p32^{-/-}$ MEFs rescued the growth retardation, indicating that p32 is important for normal cell proliferation.

Cells depleted of mtDNA would require high glucose, pyruvate and uridine for proliferation. To determine whether the addition of high glucose, pyruvate or uridine could rescue the proliferation of $p32^{-/-}$ MEFs, we added each of these supplements separately. Only pyruvate (1 mM) was able to rescue the proliferation of $p32^{-/-}$ MEFs (Figure 2E, lower panel); addition of high glucose (3500 mg/l) and uridine (0.2 mM) did not rescue

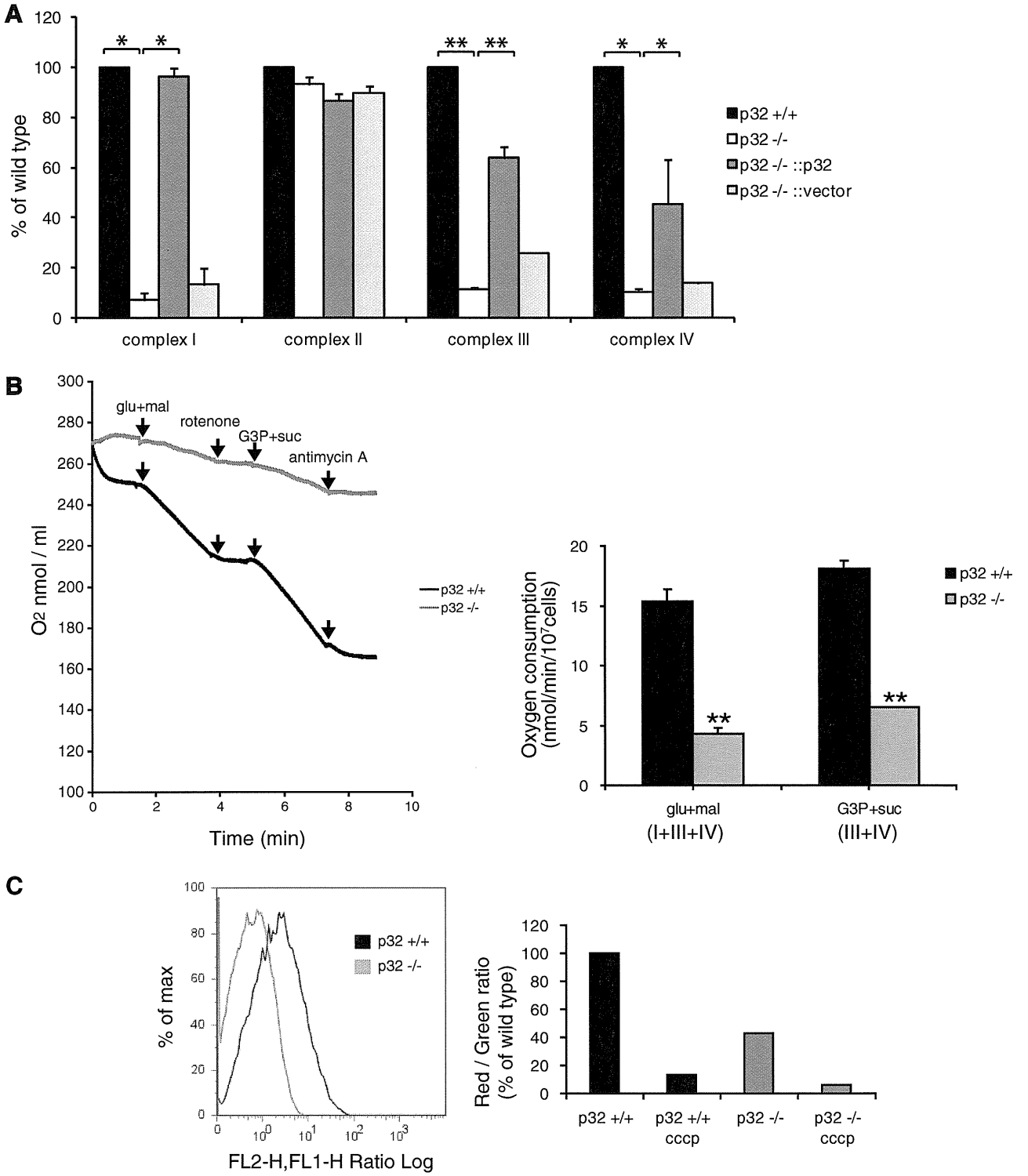

Figure 2. Reduced mitochondrial respiratory activities in $p32^{-/-}$ MEFs. (**A**) The activity of each complex was measured using cell lysates as described in 'Materials and Methods' section. Reduced enzymatic activities of mitochondrial complexes I, III and IV in p32-knockout cells were observed. In contrast, complex II activity was not decreased. Re-expression of p32 in $p32^{-/-}$ cells restored the enzymatic activities of complexes I, III and IV. The results represent the mean ± SD of three independent experiments. $^{*}P < 0.05$; $^{**}P < 0.01$ versus controls ($p32^{+/+}$ versus $p32^{-/-}$ and $p32^{-/-}$ versus $p32^{-/-}$::p32). (**B**) Oxygen consumption by digitonin-permeabilized wild-type ($p32^{+/+}$) and knockout ($p32^{-/-}$) MEFs. Glutamate and malate (glu+mal) respiration depends on the activities of complexes I, III and IV; glycerol-3-phosphate and succinate (G3P+suc) respiration depends on the activities of complexes III and IV. Rotenone (a complex I inhibitor) and Antimycin A (a complex III inhibitor) completely inhibit O_2 consumption at each step. Data show the mean ± SD of triplicate experiments and $^{**}P < 0.01$ versus controls ($p32^{+/+}$ versus $p32^{-/-}$). (**C**) Decreased mitochondrial membrane potential in p32-knockout MEFs. MEFs were stained with the fluorescent dye JC-1 and then analyzed by flow cytometry at 527 and 590 nm. The fluorescence ratio of JC1 dimer (Red)/JC-1 monomer (Green) is shown. Dissipation of the membrane potential with CCCP was used as a control.

(continued)

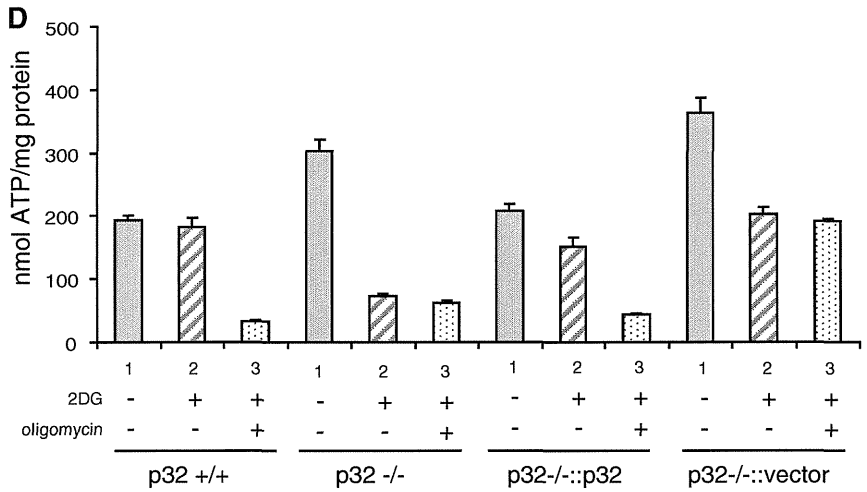

	p32 +/+	p32 -/-	p32 -/- :: p32	p32 -/- :: vector
Total ATP(lane1)	387.7	607.4	417.0	725.4
Glycolysis ATP(lane1-2)	23.9	462.2	114.6	320.9
Mitochondrial ATP(lane2-3)	297.6	20.6	213.5	20.8

(nmol ATP/mg protein)

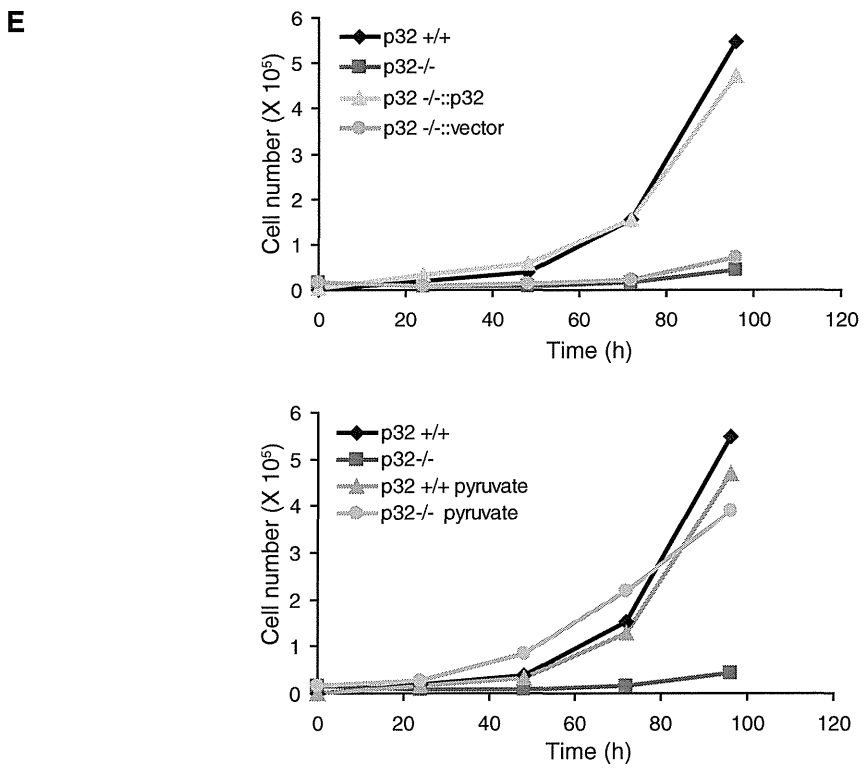

Figure 2. Continued

(**D**) Effects of 2-deoxy-D-glucose (2DG) (20 mM) and oligomycin (10 μM) on intracellular ATP content in MEFs. The ATP content in untreated MEFs is presented in lane 1. The ATP concentration of untreated MEFs (lane 1) was subtracted from that of 2DG-treated MEFs (lane 2) for assessment of glycolytic ATP production (lanes 1 and 2). The ATP concentration in 2DG-treated cells (lane 2) was subtracted from that in cells treated with 2DG + oligomycin (lane 3) for mitochondrial ATP production (lanes 2–3). Wild-type ($p32^{+/+}$), p32-knockout ($p32^{-/-}$), re-expressed p32 ($p32^{-/-}$::*p32*) and vector only-transfected ($p32^{-/-}$::vector) MEFs were used. The ATP response was measured using a Luminescence ATP assay kit in a 96-well plate. Data show the mean ± SD of triplicate experiments. (**E**) Cell proliferation monitored in MEFs. Upper panel: the diamonds, squares, triangles and circles represent wild-type MEFs ($p32^{+/+}$), p32-knockout MEFs ($p32^{-/-}$), knockout MEFs with reintroduced *p32* cDNA ($p32^{-/-}$::*p32*) and knockout MEFs with introduced vector-only cDNA ($p32^{-/-}$::vector), respectively. Lower panel: pyruvate (1 mM) was added to wild-type and $p32^{-/-}$ MEFs. The cell number was counted at 24, 48, 72 and 96 h after seeding. Here, we used DMEM (1000 mg/l glucose) supplemented with 10% dialyzed FBS without pyruvate.

proliferation (data not shown). Taken together with no decrease of cellular ATP in $p32^{-/-}$ MEFs (Figure 2D), these results suggest that impaired regeneration of NAD^+ (probably by complex I) is particularly critical for the retardation of $p32^{-/-}$ MEF proliferation.

No decreased mtDNA copy number and RNA expression

We measured the mtDNA copy number because the observed defects were likely related to mtDNA. The normal copy number of mtDNA was confirmed by qPCR, which excluded defects of mtDNA replication and/or repair as a cause of compromised protein synthesis (Figure 3A). To determine whether p32 affected the transcription of mtDNA, total RNA was isolated from cells and was assessed by qRT–PCR (Figure 3B). The steady-state level of 12S and 16S rRNA did not show a significant change between wild-type and $p32^{-/-}$ MEFs. No mtDNA-encoded mRNAs showed a decrease in p32-knockout MEFs compared with those in wild-type cells, although the levels of *ND1* and *ND6* transcripts were increased two-fold in knockout cells. The RNA expression levels in p32-re-expressed cells were also not significantly changed compared with those in wild-type cells (Figure 3B). Thus, p32 knockout did not cause a decrease in mtDNA-encoded transcripts. These results suggest that p32 deficiency does not affect the amounts of mtDNA or mRNAs.

Knockout of p32 decreases mitochondria- and nuclear-encoded proteins in mitochondria

mtDNA encodes 13 polypeptides/subunits of the mitochondrial electron respiratory chain. To determine why depletion of p32 caused a respiratory defect, we measured the expression of several members of the

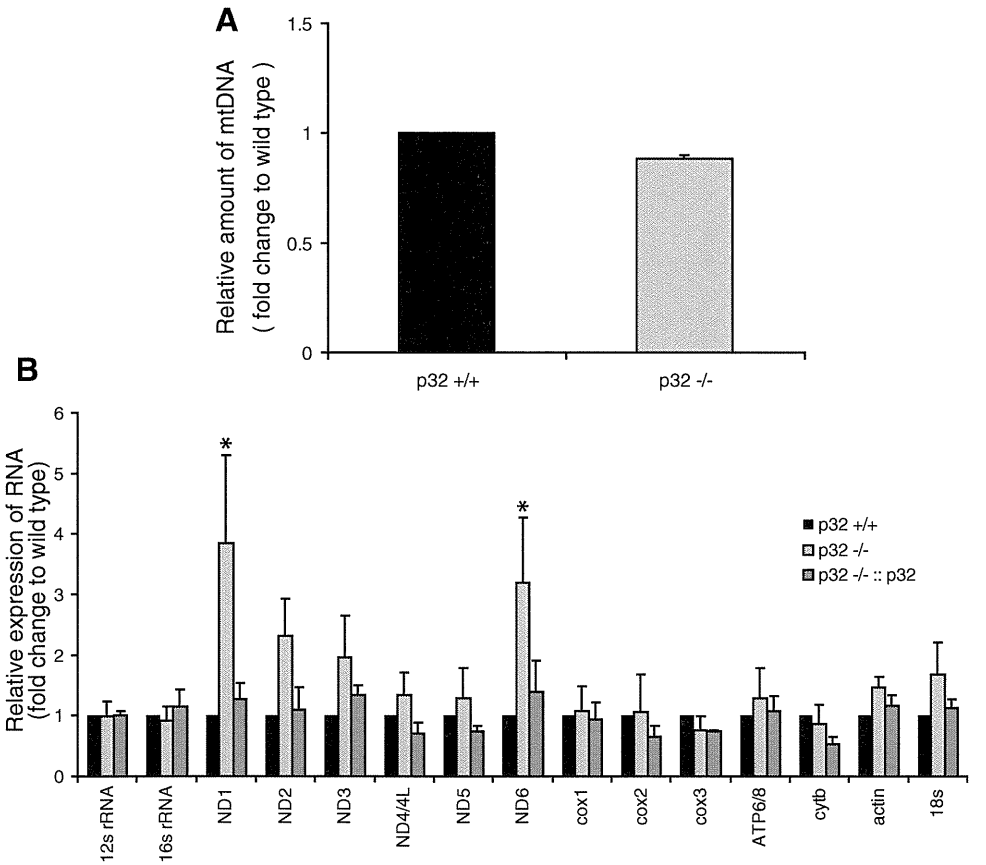

Figure 3. MtDNA copy number, RNA and protein expression in $p32^{-/-}$ MEFs. (**A**) The amount of mtDNA per cell was estimated based on the ratio of mtDNA/nuclear (n)DNA (ND2/AT-III). The relative mtDNA amount between $p32^{-/-}$ and $p32^{+/+}$ cells is shown. (**B**) Real-time PCR quantification of mitochondrial gene transcript levels isolated from wild-type ($p32^{+/+}$) MEFs, p32-knockout ($p32^{-/-}$) MEFs, and knockout MEFs with reintroduced *p32* cDNA ($p32^{-/-}$::*p32*). Two nuclear-encoded RNA species (*β-actin* and *18S* rRNA) were also quantified. Data were normalized to the expression level in wild-type $p32^{+/+}$ MEFs for each RNA species. Data show the mean ± SD of triplicate experiments and $*P < 0.05$; versus controls ($p32^{+/+}$ versus $p32^{-/-}$). (**C**) Expression of mitochondrial proteins. Crude mitochondria were prepared from equal amounts of MEFs. Ten micrograms of protein for each sample was loaded. Blots were incubated with the indicated antibodies. Lane 1, wild-type MEFs; lane 2, p32-knockout MEFs; lane 3, knockout MEFs with reintroduced *p32* cDNA; lane 4, knockout MEFs with introduced vector-only cDNA. Mt: OXPHOS protein encoded by mitochondria DNA; N: OXPHOS protein encoded by the nucleus. (**D**) *In vivo* mitochondrial translation was performed for 60 min using the cell lysates. The products were labeled during the reaction with a mixture of [^{35}S]-methionine and [^{35}S]-cysteine in the presence of emetine and/or chloramphenicol, and then detected by autoradiography after SDS–PAGE (upper panel). Deficient translation was observed in p32-knockout cells (lane 3). Equal loading was confirmed by CBB staining following exposure (lower panel). Lanes 1 and 2, wild-type MEFs; lane 3, p32-knockout MEFs; lane 4, knockout MEFs with reintroduced *p32* cDNA; lane5, knockout MEFs with introduced p32::K89A/K93A mutant; lane 6, knockout MEFs with vector-only cDNA. The protein indicated are representative proteins based on their molecular weight.

(continued)